THE VITAL ROLE OF GRADIENT CLIPPING IN BYZANTINE-RESILIENT DISTRIBUTED LEARNING

Anonymous authors
Paper under double-blind review

ABSTRACT

Byzantine-resilient distributed machine learning seeks to achieve robust learning performance in the presence of misbehaving or adversarial workers. While state-of-the-art (SOTA) robust distributed gradient descent (Robust-DGD) methods were proven theoretically optimal, their empirical success has often relied on pre-aggregation *gradient clipping*. However, the currently considered *static* clipping strategy exhibits mixed results: improving robustness against some attacks while being ineffective or detrimental against others. We address this gap by proposing a principled *adaptive* clipping strategy, termed Adaptive Robust Clipping (ARC). We show that ARC consistently enhances the empirical robustness of SOTA Robust-DGD methods, while preserving the theoretical robustness guarantees. Our analysis shows that ARC provably improves the asymptotic convergence guarantee of Robust-DGD in the case when the model is well-initialized. We validate this theoretical insight through an exhaustive set of experiments on benchmark image classification tasks. We observe that the improvement induced by ARC is more pronounced in highly heterogeneous and adversarial settings.

1 INTRODUCTION

Distributed machine learning, a.k.a. federated learning, has emerged as a dominant paradigm to cope with the increasing computational cost of learning tasks, mainly due to growing model sizes and datasets (Kairouz et al., 2021). *Worker* machines, holding each a fraction of the training dataset, collaborate over a network to learn an optimal common model over the collection of their datasets. Workers typically collaborate with the help of a central coordinator, that we call *server* (McMahan et al., 2017). Besides scalability, distributed learning is also helpful in preserving data ownership and sovereignty, since the workers do not have to share their local datasets during the learning.

Conventional distributed learning algorithms are known to be vulnerable to misbehaving workers that could behave unpredictably (Blanchard et al., 2017; Kairouz et al., 2021; Guerraoui et al., 2023). Misbehavior may result from software and hardware bugs, data poisoning, or malicious players controlling part of the network. In the parlance of distributed computing, misbehaving workers are referred to as *Byzantine* (Lamport et al., 1982). Due to the growing influence of distributed learning in critical public-domain applications such as healthcare (Nguyen et al., 2022) and finance (Long et al., 2020), the problem of robustness to misbehaving workers, a.k.a. robust distributed learning, has received significant attention (Blanchard et al., 2017; Yin et al., 2018; Farhadkhani et al., 2022; Karimireddy et al., 2022; Gorbunov et al., 2023; Allouah et al., 2023a; Farhadkhani et al., 2023).

Robust distributed learning algorithms primarily rely on robust aggregation, such as coordinate-wise trimmed mean (CWTM) (Yin et al., 2018), geometric median (GM) (Chen et al., 2017) and multi-Krum (MK) (Blanchard et al., 2017). Specifically, in robust distributed gradient descent (*Robust-DGD*), the server aggregates the workers' local gradients using a robust aggregation method, instead of simply averaging them. This protects the learning procedure from erroneous gradients sent by misbehaving workers. Recent work has made significant improvements over these aggregation rules by incorporating a pre-aggregation step such as bucketing (Karimireddy et al., 2022; Gorbunov et al., 2023) and nearest-neighbor mixing (NNM) (Allouah et al., 2023a), to tackle gradient dissimilarity resulting from data heterogeneity. The learning guarantee of the resulting Robust-DGD has been proven to be optimal (Allouah et al., 2023b), i.e., it cannot be improved without additional assumptions under the standard heterogeneity model of (G, B)-gradient dissimilarity (Karimireddy et al., 2020).

Despite its theoretical tightness, the empirical success of Robust-DGD has unknowingly relied on pre-aggregation *gradient clipping* (Mhamdi et al., 2021; Farhadkhani et al., 2022; Allouah et al., 2023a). Specifically, clipping the gradients of the workers prior to aggregation has been observed to sometimes enhance the algorithm's empirical performance in the presence of adversarial workers, as evidenced in Figure 1a. Yet, this improvement lacks a concrete explanation, raising the question of whether the observed benefits of clipping are merely anecdotal. This leads to the natural inquiry: *Why, and when, does pre-aggregation clipping improve robustness?*

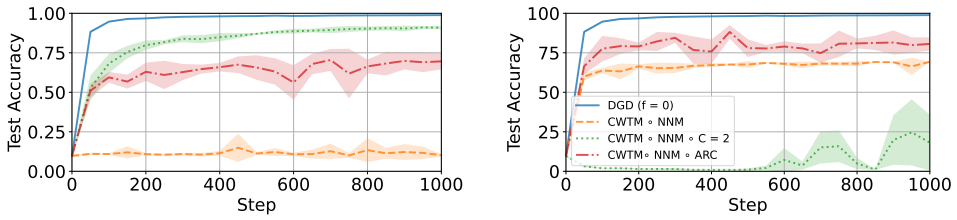

(a) Sign-flipping (SF) (Allen-Zhu et al., 2020) (b) Label-flipping (LF) (Allen-Zhu et al., 2020)

Figure 1: Impact of pre-aggregation clipping, specifically static clipping with $C = 2$ and our adaptive clipping algorithm ARC, on Robust-DGD with aggregation scheme CWTM $\circ$ NNM, under the SF and LF adversarial attacks. We consider the MNIST (Deng, 2012) dataset distributed amongst 10 honest (non-adversarial) workers with *extreme* heterogeneity, and there are three adversarial workers.

In particular, using a constant clipping threshold, referred to as static clipping, has exhibited mixed results. Figure 1 shows that while static clipping effectively mitigates sign-flipping (SF) attacks, it completely fails under label-flipping (LF). This indicates an inherent fragility of static clipping. Indeed, we prove in our work that static clipping breaks the standard (f, κ)-robustness property of an aggregation method (Allouah et al., 2023a). This highlights a key shortcoming of existing empirical results that rely on static clipping (Mhamdi et al., 2021; Farhadkhani et al., 2022; Allouah et al., 2023a). To overcome the limitations of static clipping but preserve its empirical benefits at the same time, we introduce a novel adaptive clipping scheme, termed Adaptive Robust Clipping (ARC).

ARC dynamically adjusts the clipping threshold as per the gradients sent by the workers and the fraction of adversarial workers to be tolerated. We demonstrate that integrating ARC into Robust-DGD consistently improves its empirical performance (see Figures 1 and 2a), while also preserving the convergence guarantee of the original Robust-DGD algorithm. Moreover, we show that when the model initialization is good, ARC provably improves the robustness of Robust-DGD. The benefits of ARC are more pronounced as the fraction of misbehaving workers approaches the system's breakdown point[1] and when the data across the workers is highly heterogeneous. Our key results are summarized below. Critical comparisons to prior work are deferred to Section 6.

Main results & contributions. We consider a system comprising n workers and a server. The goal is to tolerate up to f adversarial workers.

(1) Adaptive robust clipping (ARC). We propose ARC, wherein prior to aggregating the gradients, the server clips the largest $k := \lfloor 2(f/n)(n-f) \rfloor$ gradients using a clipping parameter given by the (Euclidean) norm of the $(k+1)$-th largest gradient. It is important to note that in contrast to existing adaptive clipping schemes (Diakonikolas et al., 2020; Abdalla & Zhivotovskiy, 2024), ARC does not require additional a priori information on honest workers' gradients. We prove that ARC preserves the robustness guarantee of the original robust aggregation method.

(2) Improved empirical robustness. We conduct experiments on MNIST (Deng, 2012), Fashion-MNIST (Xiao et al., 2017), and CIFAR-10 (Krizhevsky et al., 2014), across various data heterogeneity settings and adversarial regimes. Our results demonstrate that ARC significantly enhances the performance of state-of-the-art Robust-DGD methods, particularly in scenarios with high data heterogeneity (Figure 2a) and a large number of adversarial workers (Figure 4b).

(3) Improved learning guarantee. We demonstrate that ARC possesses an additional property, we call Bounded Aggregation Output, that is not satisfied by classical robust aggregation methods.

[1]Breakdown point refers the minimum fraction of adversarial workers that can break the system, making it impossible to guarantee a bound on the learning error Allouah et al. (2023b).

Specifically, ARC constrains the norm of an adversarial gradient by that of an honest (non-adversarial) gradient. Leveraging this property, we show that the lower bound established under data heterogeneity in Allouah et al. (2023b) can be circumvented using ARC, provided the honest workers' gradients are bounded at model initialization. An empirical validation of this insight is shown in Figure 2b. Such model initialization is often satisfiable in practice (Glorot & Bengio, 2010), highlighting the practical relevance of ARC. When the model is arbitrarily initialized, ARC recovers the original convergence guarantee of Robust-DGD in the worst case (see Figure 2b).

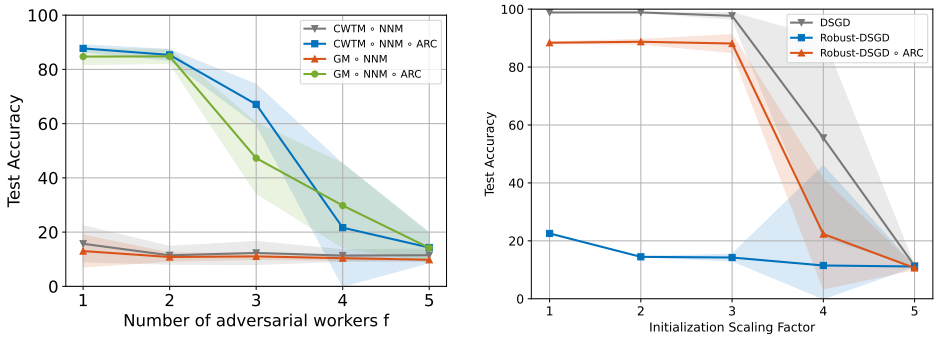

(a) Improved robustness

(b) Influence of model initialization

Figure 2: *Worst-case maximal accuracies* of Robust-DSGD, with and without ARC, across several types of misbehavior for distributed MNIST with 10 honest workers and under *extreme* heterogeneity. On the left, we vary the number of adversarial workers. On the right, we vary the initialization conditions by scaling a well-chosen set of initial parameters (CWTM $\circ$ NNM is used, and $f = 1$). More details on the experimental setup can be found in Sections 4 and 5.2, and Appendix D.

2 Problem Statement and Relevant Background

We consider the problem of distributed learning in the server-based architecture. The system comprises n workers represented by $w_1, \ldots, w_n$, that collaborate with the help of a trusted server. The workers hold local datasets $\mathcal{D}_1, \ldots, \mathcal{D}_n$ respectively, each composed of m data points from an input space $\mathcal{Z}$. Specifically, for any $i \in [n]$, $\mathcal{D}_i := \{z_1^{(i)}, \ldots, z_m^{(i)}\} \subset \mathcal{Z}^m$. For a given model parameterized by vector $\theta \in \mathbb{R}^d$, d being the number of trainable parameters in the model, each worker w_i incurs a loss given by the loss function $\mathcal{L}_i(\theta) := \frac{1}{m}\sum_{k=1}^{m} \ell(\theta, z_k^{(i)})$, where $\ell : \mathbb{R}^d \times \mathcal{Z} \to \mathbb{R}$ is the point-wise loss. We make the following standard assumptions (Bottou et al., 2018): (i) the point-wise loss function ℓ is differentiable with respect to θ. (ii) For all $i \in [n]$, $\mathcal{L}_i$ is L-Lipschitz smooth, i.e., there exists $L \in \mathbb{R}^+$ such that all $\theta, \theta' \in \mathbb{R}^d$, $\|\nabla \mathcal{L}_i(\theta) - \nabla \mathcal{L}_i(\theta')\| \leq L \|\theta - \theta'\|$, where $\|\cdot\|$ refers to the Euclidean norm. In the ideal setting where all workers are assumed to be *honest*, i.e., follow the prescribed algorithm correctly, the server aims to minimize the global average loss function given by $\mathcal{L}(\theta) := \frac{1}{n}\sum_{i=1}^{n} \mathcal{L}_i(\theta)$. However, this objective is rendered vacuous when some workers could be adversarial, described in the following.

A robust distributed learning algorithm aims to output a good model despite the presence of adversarial (a.k.a., *Byzantine* (Lamport et al., 1982)) workers in the system (Su & Vaidya, 2016; Yin et al., 2018; Allouah et al., 2023a). Specifically, the goal is to design a distributed learning algorithm that can tolerate up to f adversarial workers, of a priori unknown identity, out of n workers. Adversarial workers need not follow a prescribed algorithm, and can send arbitrary information to the server. In the context of distributed gradient descent, adversarial workers can send incorrect gradients to the server (Baruch et al., 2019; Allen-Zhu et al., 2020; Xie et al., 2020; Karimireddy et al., 2022). We let $\mathcal{H} \subseteq [n]$, with $|\mathcal{H}| = n - f$, denote the set of honest workers that do not deviate from the algorithm. The objective of the server is to minimize the average loss function of honest workers given by

$$\mathcal{L}_{\mathcal{H}}(\theta) := \frac{1}{|\mathcal{H}|}\sum_{i \in \mathcal{H}} \mathcal{L}_i(\theta), \ \forall \theta \in \mathbb{R}^d.$$

While we can find a minimum of $\mathcal{L}_{\mathcal{H}}(\theta)$ when $\mathcal{L}_{\mathcal{H}}$ is convex, in general however the loss function is non-convex, and the optimization problem is NP-hard (Boyd & Vandenberghe, 2004). Therefore, we aim to find a *stationary point* of $\mathcal{L}_{\mathcal{H}}$ instead, i.e., θ^* such that $\|\nabla \mathcal{L}_{\mathcal{H}}(\theta^*)\| = 0$. Formally, we define robustness to adversarial workers by (f, ϵ)-*resilience* (Allouah et al., 2023a).

Definition 2.1. A distributed learning algorithm $\mathcal{A}$ is said to be (f, ε)-*resilient* if, despite the presence of f adversarial workers, $\mathcal{A}$ enables the server to output a model $\hat{\theta}$ such that $\mathbb{E}\left[\left\|\nabla \mathcal{L}_{\mathcal{H}}\left(\hat{\theta}\right)\right\|^2\right] \leq \varepsilon$, where the expectation $\mathbb{E}\left[\cdot\right]$ is over the randomness of the algorithm.

If a distributed learning algorithm $\mathcal{A}$ is (f, ε)-resilient then it can tolerate up to f adversarial workers. It is standard in robust distributed learning to design robust algorithms using f as a parameter (Su & Vaidya, 2016; Blanchard et al., 2017; Yin et al., 2018; Karimireddy et al., 2022; Gorbunov et al., 2023; Allouah et al., 2023a), f being the maximum tolerable number of adversarial workers.

In the context of distributed learning, data heterogeneity is characterized by the following standard notion of (G, B)-gradient dissimilarity (Vaswani et al., 2019; Karimireddy et al., 2020; 2022; Gorbunov et al., 2023; Allouah et al., 2023b).

Definition 2.2. Loss functions $\mathcal{L}_i,\ i \in \mathcal{H}$, are said to satisfy (G, B)-*gradient dissimilarity* if,

$$\frac{1}{|\mathcal{H}|} \sum_{i \in \mathcal{H}} \|\nabla \mathcal{L}_i(\theta) - \nabla \mathcal{L}_{\mathcal{H}}(\theta)\|^2 \leq G^2 + B^2 \|\nabla \mathcal{L}_{\mathcal{H}}(\theta)\|^2, \quad \forall \theta \in \mathbb{R}^d.$$

General limitations on robustness. Note that (f, ε)-resilience is impossible (for any ε) when $f/n \geq 1/2$ (Gupta & Vaidya, 2020). Moreover, even for $f/n < 1/2$, it is generally impossible to achieve (f, ε)-resilience for arbitrarily small ε due to the disparity amongst the local datasets $\mathcal{D}_i,\ i \in \mathcal{H}$ (a.k.a., data heterogeneity) (Liu et al., 2021). Henceforth, we assume that $n > 2f$. Under (G, B)-gradient dissimilarity, we have the following lower bound on the achievable resilience.

Lemma 2.3 (Non-convex extension of Theorem 1 Allouah et al.)**.** *Under (G, B)-gradient dissimilarity, a distributed learning algorithm is (f, ε)-resilient only if $\frac{f}{n} < \frac{1}{2+B^2}$ and $\varepsilon \geq \frac{1}{4} \cdot \frac{f}{n-(2+B^2)f} G^2$.*

For a given distributed learning problem, the minimum fraction of adversarial workers that renders any distributed learning algorithm ineffective is called the *breakdown point* (Guerraoui et al., 2023; Allouah et al., 2023b). Thus, according to Lemma 2.3, there exists a distributed learning problem satisfying (G, B)-gradient dissimilarity whose breakdown point is given by $1/(2 + B^2)$.

Robust distributed gradient descent. To tolerate adversarial workers, we replace the averaging operation in the classic distributed gradient descent (DGD) method with a robust aggregation, e.g., coordinate-wise trimmed mean (CWTM) and median (CWMed) (Yin et al., 2018), geometric median (GM) (Chen et al., 2017), and multi-Krum (MK) (Blanchard et al., 2017). This yields Robust-DGD, presented in Algorithm 1, where robust aggregation protects the learning from incorrect gradients sent by the adversarial workers. The robustness of an aggregation method can be quantified by the following property of (f, κ)-robustness, proposed by Allouah et al. (2023a).

Algorithm 1 Robust Distributed Gradient Descent (Robust-DGD)

Initialization: **Server** chooses a model $\theta_1 \in \mathbb{R}^d$, a learning rate $\gamma \in \mathbb{R}^+$ and a robust aggregation method $\mathbf{F} : \mathbb{R}^{n \times d} \to \mathbb{R}^d$.
for $t = 1$ to T **do**
  Server broadcasts θ_t to all workers.
  for each honest worker w_i **in parallel do**
    Compute local gradient $g_t^{(i)} := \nabla \mathcal{L}_i(\theta_t)$, and send $g_t^{(i)}$ to **Server**.
    // An adversarial worker w_j can send an arbitrary vector in $\mathbb{R}^d$ for $g_t^{(j)}$
  end for
  Server computes $R_t := \mathbf{F}\left(g_t^{(1)}, \ldots, g_t^{(n)}\right)$.
  Server computes the updated model $\theta_{t+1} := \theta_t - \gamma R_t$.
end for
Output: **Server** outputs $\hat{\theta}$ chosen uniformly at random from $\{\theta_1, \ldots, \theta_T\}$.

Definition 2.4. $\mathbf{F} : \mathbb{R}^{n\times d} \to \mathbb{R}^d$ is said to be (f,κ)-*robust* if there exists a robustness coefficient $\kappa \in \mathbb{R}$ such that for all $x_1,\ldots,x_n \in \mathbb{R}^d$ and any set $S \subseteq [n]$, $|S| = n-f$, the following holds:

$$\left\|\mathbf{F}(x_1,\ldots,x_n) - \overline{x}_S\right\|^2 \leq \frac{\kappa}{|S|}\sum_{i\in S}\left\|x_i - \overline{x}_S\right\|^2 \quad , \quad \text{where } \overline{x}_S = \frac{1}{|S|}\sum_{i\in S} x_i.$$

(f,κ)-robustness[2] encompasses several robust aggregations, including the ones mentioned above and more (e.g., see Allouah et al. (2023a)). It has been shown that an aggregation method is (f,κ)-robust only if $\kappa \geq \frac{f}{n-2f}$ (Allouah et al., 2023a). Importantly, the asymptotic error of Robust-DGD with (f,κ)-robust aggregation, where $\kappa \in \mathcal{O}(f/(n-2f))$, matches the lower bound (recalled in Lemma 2.3) (Allouah et al., 2023b). Note that the aforementioned aggregation methods (CWTM, CWMed, GM and MK) attain optimal robustness when composed with the pre-aggregation scheme: nearest neighbor mixing (NNM) (Allouah et al., 2023a).[3] Specifically, we recall the following result.

Lemma 2.5 (Lemma 1 in Allouah et al. (2023a))**.** *For* $\mathbf{F} \in \{\mathbf{CWTM}, \mathbf{CWMed}, \mathbf{GM}, \mathbf{MK}\}$*, the composition* $\mathbf{F}\circ\mathbf{NNM}$ *is* (f,κ)*-robust with*

$$\kappa \leq \frac{8f}{n-f}\left(1 + \left(1 + \frac{f}{n-2f}\right)^2\right).$$

Thus, if $n \geq (2+\delta)f$ for $\delta > 0$, then $\mathbf{F}\circ\mathbf{NNM}$ is (f,κ)-robust with $\kappa \leq \frac{16f}{n-f}\left(\frac{\delta+1}{\delta}\right)^2 \in \mathcal{O}\left(\frac{f}{n-2f}\right)$.

Convergence of Robust-DGD. Lastly, we recall the convergence result for Robust-DGD with an (f,κ)-robust aggregation $\mathbf{F}$. We let $\mathcal{L}^*_{\mathcal{H}}$ denote the minimum value of $\mathcal{L}_{\mathcal{H}}(\theta)$.

Lemma 2.6 (Theorem 2 in Allouah et al. (2023b))**.** *Consider Algorithm 1 with* $\gamma \leq 1/L$*. Let* $\Delta_o \in \mathbb{R}^+$ *such that* $\mathcal{L}_{\mathcal{H}}(\theta_1) - \mathcal{L}^*_{\mathcal{H}} \leq \Delta_o$*. If* $\mathbf{F}$ *is* (f,κ)*-robust with* $\kappa B^2 < 1$*, then*

$$\frac{1}{T}\sum_{t=1}^{T}\left\|\nabla\mathcal{L}_{\mathcal{H}}(\theta_t)\right\|^2 \leq \frac{2\Delta_o}{(1-\kappa B^2)\gamma T} + \frac{\kappa G^2}{1-\kappa B^2}.$$

Thus, when $\kappa \in \mathcal{O}\left(f/(n-2f)\right)$ (and smaller than $1/B^2$), Robust-DGD is optimal, i.e., its error matches the lower bound recalled in Lemma 2.3, as soon as $T \geq \Delta_o/\gamma\kappa G^2$.[4]

3 Adaptive Robust Clipping (ARC) and its Properties

In this section, we first present a preliminary observation on the fragility of *static* clipping, and then introduce *adaptive* robust clipping (i.e., ARC) along with its robustness guarantees.

For a clipping parameter $C \in \mathbb{R}^+$ and a vector $x \in \mathbb{R}^d$, we denote $\mathrm{clip}_C(x) \coloneqq \min\left(1, \frac{C}{\|x\|}\right)x$. For a set of n vectors $x_1,\ldots,x_n \in \mathbb{R}^d$, we denote $\mathbf{Clip}_C(x_1,\ldots,x_n) \coloneqq (\mathrm{clip}_C(x_1),\ldots,\mathrm{clip}_C(x_n))$.

Let $\mathbf{F}$ be an (f,κ)-robust aggregation. Given a set of n vectors $x_1,\ldots,x_n$, let $\mathbf{F}\circ\mathbf{Clip}_C(x_1,\ldots,x_n) \coloneqq \mathbf{F}\left(\mathbf{Clip}_C(x_1,\ldots,x_n)\right)$. We make the following observation.

Lemma 3.1. *For any fixed* $C \in \mathbb{R}^+$ *and* $\kappa' \geq 0$*,* $\mathbf{F}\circ\mathbf{Clip}_C$ *is not* (f,κ')*-robust.*

Thus, if the clipping threshold is fixed, i.e., independent from the input vectors, pre-aggregation clipping does not preserve the robustness of the original aggregation. This fragility of such *static* clipping is also apparent in practice, as shown by our experimental study in Appendix F (and Figure 1).

Description of ARC. ARC is an adaptive clipping scheme that only makes use of the standard robustness parameter f/n, i.e., the tolerable fraction of adversarial workers. ARC is *adaptive* in the sense that the clipping threshold C is not fixed but depends on the input vectors. Specifically, ARC clips the largest $k = \lfloor 2(f/n)(n-f)\rfloor$ vectors using a clipping parameter given by the norm of the $(k+1)$-th largest input vector. The overall scheme is formally presented in Algorithm 2, and its computational complexity is $\mathcal{O}(nd + n\log(n))$ (see Appendix A). Thus, pre-composing more computationally expensive schemes like NNM and multi-Krum, which have a complexity of $\mathcal{O}(dn^2)$, with ARC does not introduce a significant overhead.

Robustness Guarantee. We present below the preservation of robustness guaranteed by ARC. Let $\mathbf{F}$ be an (f,κ)-robust aggregation rule and $\mathbf{F}\circ\mathbf{ARC}(x_1,\ldots,x_n) \coloneqq \mathbf{F}(\mathbf{ARC}(x_1,\ldots,x_n))$.

[2]Unifies $(\delta_{\max}, c)$-robustness (Karimireddy et al., 2021) and (f,λ)-resilience (Farhadkhani et al., 2022).

[3]CWTM has been shown to be optimal even without NNM.

[4]For $f = 0$, Lemma 2.3 recovers the convergence of DGD, provided that κ is tight, i.e., $\kappa \in \mathcal{O}(f/(n-2f))$.

Algorithm 2 Adaptive Robust Clipping (ARC)

Input: f and $x_1, \ldots, x_n \in \mathbb{R}^d$.
Find a permutation $\pi : [n] \to [n]$ such that $\left\|x_{\pi(1)}\right\| \geq \left\|x_{\pi(2)}\right\| \ldots \geq \left\|x_{\pi(n)}\right\|$.
Set $k = \left\lfloor 2\frac{f}{n}(n-f) \right\rfloor$ and $C = \left\|x_{\pi(k+1)}\right\|$.
Output: $\mathbf{Clip}_C(x_1, \ldots, x_n)$.

Theorem 3.2. *If* $\mathbf{F}$ *is* (f, κ)*-robust, then* $\mathbf{F} \circ \mathbf{ARC}$ *is* $\left(f, \kappa + \frac{2f}{n-2f}\right)$*-robust.*

Proofs for the results presented in this section are deferred to Appendix B. Since $\kappa \geq \frac{f}{n-2f}$ (recalled in Section 2), Theorem 3.2 implies that $\mathbf{F} \circ \mathbf{ARC}$ is $(f, 3\kappa)$-robust. In other words, ARC preserves the robustness of the original aggregation scheme. Therefore, a convergence result for Robust-DGD with ARC follows verbatim from Lemma 2.6, replacing κ with 3κ. Despite this multiplicative factor of 3, we observe in the next section that incorporating ARC consistently improves the empirical performance of classical aggregation methods. A more detailed theoretical explanation will be provided later in Section 5.1.

4 Empirical Evaluation

In this section, we delve into the practical performance of ARC when incorporated in Robust-D*S*GD (Algorithm 3 in Appendix D), an order-optimal *stochastic* variant of Robust-DGD (Allouah et al., 2023a). We conduct experiments on standard image classification tasks, covering different adversarial scenarios. We empirically test four aggregation methods when pre-composed with ARC. We also contrast these outcomes against the performance of Robust-DSGD when no gradient clipping is used. Our findings underscore that clipping workers' gradients using ARC prior to the aggregation is crucial to ensure the robustness of existing algorithms, especially in extreme scenarios, i.e., when either the data heterogeneity is high or the fraction of adversarial workers is large.

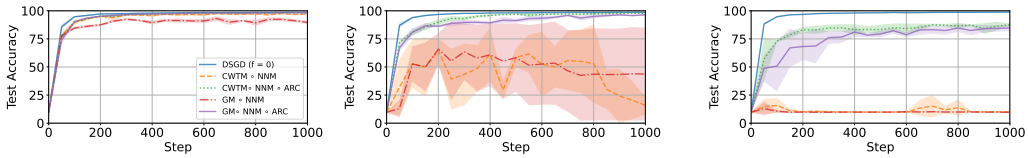

(a) $\alpha = 0.5$ (b) $\alpha = 0.1$ (c) extreme heterogeneity

Figure 3: Performance of Robust-DSGD when using ARC and without clipping on MNIST. There are 10 honest workers and $f = 1$ adversarial worker executing **FOE** (Xie et al., 2020).

We show in Table 1, and Figures 2a and 4, the metric of *worst-case maximal accuracy*. For each of the five *Byzantine attacks* executed (see Appendix D.3), we record the maximal accuracy achieved by Robust-DSGD during the learning procedure under that attack. The *worst-case maximal accuracy* is thus the *smallest* maximal accuracy reached across the five attacks. As the attack cannot be known in advance, this metric is critical to accurately evaluate the robustness of aggregation methods, since it provides an estimate of the potential worst-case performance of the algorithm. Furthermore, we use the Dirichlet (Hsu et al., 2019a) distribution of parameter α to simulate data heterogeneity. The comprehensive experimental setup can be found in Appendix D. In this section, we focus on presenting our results for the CWTM and GM aggregation methods applied to MNIST and CIFAR-10. Results for Fashion-MNIST, as well as for the CWMed and MK aggregations, are provided in Appendix E. All aggregation methods in our experiments are pre-composed with NNM (Allouah et al., 2023a), but we omit explicit mention of NNM in their names throughout the text for simplicity.

ARC boosts robustness in high heterogeneity. Figure 3 shows the performance of Robust-DSGD against the FOE attack when using ARC opposed to no clipping. In low heterogeneity (i.e., $\alpha = 0.5$, see Figure 7), the performances of ARC and no clipping are comparable for both aggregations. When the heterogeneity increases ($\alpha = 0.1$), the benefits of using ARC are more visible. CWTM and GM significantly struggle to learn (with a very large variance), while the same aggregations composed with ARC almost match the accuracy of DSGD towards the end of the training. In extreme heterogeneity, the improvement induced by our method is the most pronounced, as ARC enables both aggregations to reach a final accuracy close to 90%. Contrastingly, the same aggregations without

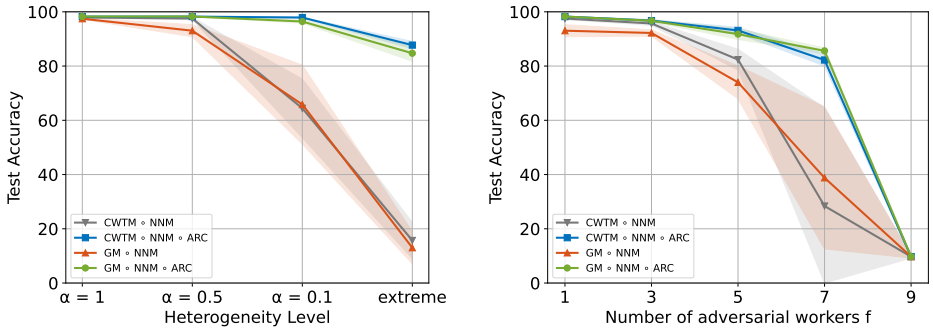

(a) $f = 1$ (b) $\alpha = 0.5$

Figure 4: *Worst-case maximal accuracies* achieved by Robust-DSGD, with and without ARC, on heterogeneously-distributed MNIST with 10 honest workers. *Left:* $f = 1$ adversarial worker among $n = 11$ for varying levels of heterogeneity. *Right:* $\alpha = 0.5$ for varying f.

clipping stagnate at around 10% throughout the training. Interestingly, only $f = 1$ adversarial worker among $n = 11$ (i.e., less than 10%) suffices to completely deteriorate the learning when no clipping is applied, highlighting the necessity of ARC in extreme heterogeneity.

Varying heterogeneity for fixed f. Figure 4a compares the worst-case maximal accuracies achieved by Robust-DSGD when $f = 1$, with ARC and without, for varying levels of heterogeneity. While CWTM and GM yield comparable accuracies with ARC in low heterogeneity ($\alpha \geq 0.5$), their performance significantly degrades when α drops below that threshold. Indeed, when $\alpha = 0.1$, their accuracies drop below 65%, while ARC enables the same aggregations to maintain their accuracy at just below 98%. In extreme heterogeneity, the performance of the aggregations without clipping completely deteriorates with accuracies close to 15%. Contrastingly, ARC efficiently mitigates the Byzantine attacks, resulting in accuracies above 85% in the worst case for both aggregations. Similar plots for $f = 3, 5, 7$ convey similar observations (see Appendix E.1). Essentially, in low heterogeneity or when the fraction of adversarial workers is small, no clipping yields good empirical results and ARC performs at least as well as no clipping. However, ARC induces a significant improvement near the breakdown point of SOTA robust aggregation schemes (e.g., high heterogeneity or large f).

ARC increases the breakdown point in adverse settings. Figure 2a of Section 1 shows that for $f \in \{1, ..., 5\}$, Robust-DSGD with CWTM and GM completely fails to learn, consistently yielding worst-case maximal accuracies close to 15%. This suggests that $f = 1$ constitutes the breakdown point for these aggregations in extreme heterogeneity. However, composing them with ARC increases the breakdown point of these aggregations to $f = 3$. Indeed, for $f = 1$ and 2, ARC enables Robust-DSGD to achieve accuracies greater than 85% in the worst case. However, when $f \geq 3$, the performance degrades, although CWTM with ARC is still able to reach a satisfactory accuracy close to 70%. Moreover, even when the heterogeneity is not large, ARC still produces a significant improvement when the fraction of adversarial workers increases in the system. Indeed, in Figure 4b , the performances of ARC and no clipping are comparable for $f \leq 3$. However, the improvement induced by ARC is much more visible when $f \geq 5$. Particularly when $f = 7$, ARC enables CWTM and GM to reach accuracies greater than 80% in the worst case, whereas the same aggregations yield accuracies below 40% without clipping . This observation indicates the raise of the breakdown point due to ARC in practice. Plots for $\alpha = 0.1$ and 1 convey the same observations in Appendix E.1.

Improved robustness on CIFAR-10. We also conduct experiments on the more challenging CIFAR-10 task with $n = 17$ and $f = 1$. Table 2 shows the worst-case maximal accuracies achieved by ARC and no clipping for four robust aggregations. For $\alpha = 0.2$, ARC consistently outputs accuracies greater than 67% for all aggregations, while the same aggregations without clipping yield lower accuracies (with a larger variance across seeds). For instance, GM achieves 41.2% on average, i.e., 26% less than its counterpart with ARC. In the more heterogeneous setting $\alpha = 0.075$, ARC enables all aggregations

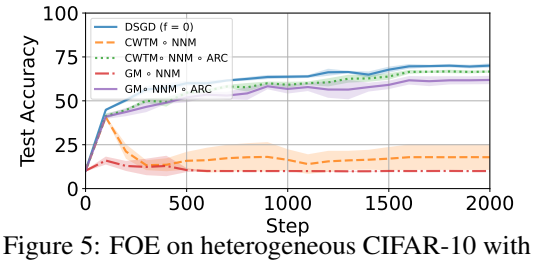

Figure 5: FOE on heterogeneous CIFAR-10 with $\alpha = 0.075$. $f = 1$ among $n = 17$.

to reach worst-case maximal accuracies close to 60% (with a small variance). However, executing the same methods without clipping significantly deteriorates the performance of Robust-DSGD, with GM and CWMed achieving 16% and 13.7% in worst-case accuracy, respectively. This can also be seen in Figure 5, where FOE completely degrades the learning when ARC is not used.

	$\alpha = 0.2$		$\alpha = 0.075$	
Aggregation	No Clipping	ARC	No Clipping	ARC
CWTM	51.6 ± 5.1	$\mathbf{67.8} \pm \mathbf{0.9}$	40.7 ± 0.5	$\mathbf{60.5} \pm \mathbf{1.2}$
GM	41.2 ± 3.5	$\mathbf{67.0} \pm \mathbf{1.0}$	16.0 ± 2.3	$\mathbf{60.0} \pm \mathbf{2.0}$
CWMed	43.4 ± 4.2	$\mathbf{69.4} \pm \mathbf{0.8}$	13.7 ± 12.1	$\mathbf{62.7} \pm \mathbf{1.2}$
MK	50.9 ± 5.1	$\mathbf{68.7} \pm \mathbf{0.5}$	40.5 ± 0.7	$\mathbf{59.9} \pm \mathbf{1.9}$

Table 1: *Worst-case maximal accuracies* (%) achieved by Robust-DSGD on heterogeneously-distributed CIFAR-10 with ARC and without. There is $f = 1$ adversarial worker among $n = 17$. As a baseline, DSGD ($f = 0$) reaches 76.5% and 70% when $\alpha = 0.2$ and 0.075, respectively.

5 Improved Guarantee of Robust-DGD with ARC

In Section 4, we empirically demonstrated that ARC outperforms SOTA aggregation methods without clipping, despite these methods being theoretically proven to be optimal. This naturally raises the question: why does ARC, which shares similar convergence guarantees, significantly outperform plain Robust-DSGD? To address this, we now focus on the influence of model initialization on the robustness of aggregation methods, considering both theoretical results and empirical insights.

5.1 Improvement of convergence guarantees

In this section, we characterize the improvement of Robust-DGD with ARC over the lower bound recalled in Lemma 2.3. Specifically, we consider Algorithm 1 with aggregation $\mathbf{F} \circ \mathbf{ARC}$, i.e., in each learning step t, $R_t \coloneqq \mathbf{F} \circ \mathbf{ARC}\left(g_t^{(1)}, \ldots, g_t^{(n)}\right)$. First, we establish in Lemma 5.1 a key property of ARC, which is crucial for deriving the improved stationarity error of Robust-DGD with ARC in Theorem 5.2.

Lemma 5.1 (**Bounded Aggregation Output**). *Let* $\mathbf{F}$ *be an* (f, κ)*-robust aggregation method. For any vectors* $x_1, \ldots, x_n \in \mathbb{R}^d$ *and set* $S \subset [n]$ *such that* $|S| = n - f$*, the following holds true:*

$$\|\mathbf{F} \circ \mathbf{ARC}(x_1, \ldots, x_n)\| \leq \max_{i \in S} \|x_i\| \tag{1}$$

This result indicates that incorporating ARC bounds the norm of the aggregated output by the largest norm of the honest gradients, i.e., $\max_{i \in \mathcal{H}} \|x_i\|$. In Appendix C, we provide the proof of Lemma 5.1 and further demonstrate in Lemma C.1 that this property is specific to ARC, i.e., classic (f, κ)-robust aggregation methods do not inherently exhibit this behavior. This property enables us to obtain the following improvement on the asymptotic convergence guarantee of Robust-DGD with ARC.

In the following, we show that when the local gradients of the honest workers at the initial model θ_1 are sufficiently small, then Robust-DGD with ARC overcomes the lower bound recalled in 2.3. For ease of presentation, we denote $\mathsf{BP} \coloneqq \frac{1}{2+B^2}$, let

$$\varepsilon_o \coloneqq \frac{1}{4} \cdot \frac{G^2(f/n)}{1 - (2 + B^2)(f/n)}, \quad \text{and} \quad \Psi(G, B, \rho) \coloneqq 640 \left(1 + \frac{1}{B^2}\right)^2 \left(1 + \frac{B^2 \rho^2}{G^2}\right),$$

where ρ denotes a real value. Recall from Lemma 2.3 that BP and ε_o are the breakdown point and the lower bound on the stationarity error when $f/n < \mathsf{BP}$, respectively, under (G, B)-gradient dissimilarity. We obtain the following theorem for Robust-DGD with ARC. Let Δ_o be a real value such that $\mathcal{L}_{\mathcal{H}}(\theta_1) - \mathcal{L}_{\mathcal{H}}^* \leq \Delta_o$. The proof of Theorem 5.2 is deferred to Appendix C.

Theorem 5.2. *Suppose* $B > 0$ *and there exists* $\zeta \in \mathbb{R}^+$ *such that* $\max_{i \in \mathcal{H}} \|\nabla \mathcal{L}_i(\theta_1)\| \leq \zeta$. *Let* $\mathbf{F} \in \{\mathbf{CWTM}, \mathbf{CWMed}, \mathbf{GM}, \mathbf{MK}\} \circ \mathbf{NNM}$ *,* $\gamma = \min\left\{\left(\frac{\Delta_o}{\kappa G^2}\right)\frac{1}{T}, \frac{1}{L}\right\}$ *and* $T \geq \frac{\Delta_o L}{\kappa G^2}$. *Consider an arbitrary real value* $\xi_o \in (0, 1)$. *Let* $\rho \coloneqq \exp\left(\frac{(2+B^2)\Delta_o}{(1-\xi_o)G^2} L\right)\zeta$. *For any* $\boldsymbol{\upsilon} \in (0, 1)$*, if* $\frac{f}{n} \coloneqq (1 - \xi)\mathsf{BP}$*, where* $0 < \xi \leq \min\left\{\frac{\boldsymbol{\upsilon}}{\Psi(G,B,\rho)}, \xi_o\right\}$*, then* $\mathbb{E}\left[\left\|\nabla \mathcal{L}_{\mathcal{H}}\left(\hat{\theta}\right)\right\|^2\right] \leq \boldsymbol{\upsilon}\, \varepsilon_o$.

Theorem 5.2 demonstrates that Robust-DGD with ARC improves over the lower bound ε_o when the ratio f/n is sufficiently close to the breakdown point (BP), provided the local gradients at model initialization are bounded. This, in turn, leads to an improvement over the original learning guarantee of Robust-DGD (as stated in Lemma 2.6), which applies for arbitrary model initialization.

Influence of model initialization and data heterogeneity. Note that the smaller the bound on the initial gradients (i.e., the better the model initialization), the greater the improvement induced by ARC. Specifically, a decrease in ζ leads to a reduction in ρ, which subsequently lowers $\Psi(G, B, \rho)$. As a result, for a fixed value of ξ (i.e., for a fixed ratio of adversarial workers), the condition $\xi \leq \boldsymbol{\upsilon}/\Psi(G, B, \rho)$ is satisfied for a smaller $\boldsymbol{\upsilon}$, thereby yielding a lower stationarity error. This theoretical deduction is empirically validated in Section 5.2. A similar improvement occurs when increasing data heterogeneity, while keeping all other factors unchanged. Specifically, as G increases, $\Psi(G, B, \rho)$ decreases, allowing for a smaller reduction factor $\boldsymbol{\upsilon}$ and thus a larger improvement in performance. This trend is also validated empirically in Figures 3 and 4a.

Influence of f/n. Additionally, for a fixed model initialization, an increase of f/n towards the BP (i.e., as $\xi \to 0$) allows the reduction factor $\boldsymbol{\upsilon}$ to become smaller, leading to a greater improvement, as evidenced in Figures 2a and 4b. Indeed, we show in Theorem C.4 (a more complete version of Theorem 5.2) that ARC effectively increases the BP of (f, κ)-robust methods from $\frac{1}{2+B^2}$ to $\frac{1}{2}$, provided the initial honest gradients are bounded in norm. Lastly, we would like to recall that when the workers' gradients at model initialization are arbitrarily large, the convergence guarantee of Robust-DGD with ARC reduces to that of classic Robust-DGD (see Section 3). In other words, there is no downside to incorporating ARC.

5.2 Influence of model initialization on empirical robustness

Figures 2b and 6 illustrate the effect of model initialization on the performance of Robust-DSGD with and without ARC, evaluated on MNIST with 10 honest workers. We investigate two regimes of heterogeneity: extreme heterogeneity and $\alpha = 0.1$, and consider $f = 1$ adversarial worker. The experiment proceeds as follows: we begin with the default model parameters initialized by PyTorch (i.e., the same ones used in Section 4), which represent a well-chosen set of initial parameters. These parameters are then scaled multiplicatively by a factor μ where larger values of μ correspond to progressively worse initialization, and vary $\mu \in \{1, ..., 5\}$. The results show that, under well-initialized conditions ($\mu = 1$), ARC significantly enhances the performance of Robust-DSGD, achieving a substantial improvement in worst-case maximal accuracy, particularly under extreme heterogeneity. In this regime, ARC boosts accuracy by about 70% compared to plain Robust-DSGD (Figure 2b). This ($\mu = 1$) corresponds to the initialization conditions of the empirical results presented in Section 4. As μ increases (i.e., the initialization worsens), the performance of ARC-enhanced Robust-DSGD gradually declines, with noticeable degradation starting from $\mu = 4$. Nevertheless, even at this point, ARC still offers a performance advantage over Robust-DSGD without clipping. By $\mu = 5$, the performance of Robust-DSGD with ARC converges to that of plain Robust-DSGD, both achieving an accuracy of around 10%. Another key observation from Figures 2b and 6 is that the behavior of Robust-DSGD with ARC closely mirrors that of Byzantine-free DSGD. Both exhibit similarly poor performance when $\mu = 5$, and their accuracies are comparable when $\mu \leq 3$, especially when $\alpha = 0.1$. This suggests that ARC is particularly effective at exploiting good model initialization, similar to the performance of DSGD in the absence of Byzantine workers. In contrast, plain Robust-DSGD struggles to fully leverage well-initialized models, as evidenced by its consistently lower accuracy (around 20%) in Figure 2b. These findings highlight the important influence of model

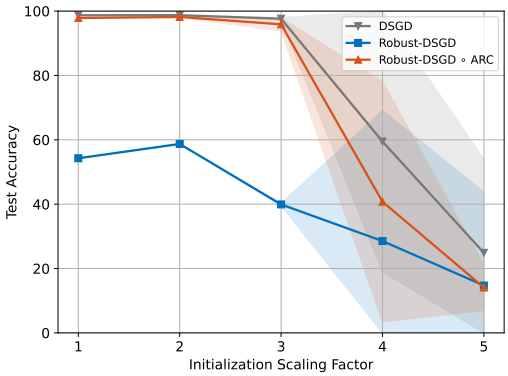

Figure 6: Worst-case maximal accuracies achieved by Robust-DSGD with CWTM, both with and without ARC, on MNIST with $\alpha = 0.1$, 10 honest worker, and $f = 1$ Byzantine worker. The x-axis represents settings with progressively worse model initialization. This figure complements Figure 2b.

initialization on the robustness of aggregation methods, and empirically validate our theoretical findings in Section 5.1.

6 Related Work

Gradient clipping is a well-known technique for tackling exploding gradients in deep learning (Goodfellow et al., 2016). It has been extensively analyzed in the centralized setting (Zhang et al., 2020b;a; Koloskova et al., 2023), with applications to differential privacy (Pichapati et al., 2019). Moreover, we would like to note that gradient clipping has also been shown useful to obtain tighter convergence guarantees for stochastic gradient-descent methods in the case where the gradients have heavy-tailed noise Gorbunov et al. (2020; 2022); Danilova (2023). The considered proof techniques, however, do not apply directly to our adversarial distributed learning setting. A similar study on the impact of clipping also exists for distributed settings (Zhang et al., 2022; Khirirat et al., 2023).

In the context of robust distributed learning, prior work has proposed *iterative* clipping for robust aggregation (Karimireddy et al., 2021). The clipping scheme, however, has not been shown to induce any improvement over other SOTA robustness schemes. Recent work (Malinovsky et al., 2023) has proposed pre-aggregation clipping using temporal gradient differences, in conjunction with variance reduction, to tackle partial worker participation when adversarial workers can form a majority. We, however, propose and study pre-aggregation clipping as a tool to improve the robustness obtained by a general class of aggregation rules. Other prior work (Mhamdi et al., 2021; Farhadkhani et al., 2022; Allouah et al., 2023a) that used static pre-aggregation clipping to enhance the empirical robustness of Robust-DGD, did not provide any formal explanation.

While adaptive clipping schemes, similar to ARC, have been proposed and studied in the context of robust aggregation (Gupta & Vaidya, 2020; Liu et al., 2021; Diakonikolas et al., 2020; Abdalla & Zhivotovskiy, 2024), critical differences should be noted. The robustness guarantees in (Gupta & Vaidya, 2020; Liu et al., 2021) only apply to strongly convex loss functions, under a specific redundancy condition (namely, $2f$*-redundancy*). We consider non-convex loss functions, as well as a generic heterogeneous setting of (G, B)-gradient dissimilarity. In contrast to the clipping scheme proposed in Diakonikolas et al. (2020); Abdalla & Zhivotovskiy (2024), ARC only uses the f/n parameter to tune the clipping threshold and does not rely on any additional a priori knowledge of the distribution of honest workers' gradients. Moreover, we prove a deterministic robustness property of ARC (see Theorem 3.2), whereas Diakonikolas et al. (2020); Abdalla & Zhivotovskiy (2024) only provide probability guarantees assuming the non-adversarial inputs to be i.i.d. with the distribution satisfying certain special properties.

7 Conclusion & Discussion

We introduced Adaptive Robust Clipping (ARC), a pre-aggregation clipping scheme designed to harness the empirical benefits of gradient clipping, while preserving the worst-case optimal convergence guarantees of Robust-DGD. Unlike existing adaptive clipping schemes, ARC does not require additional tuning since it only relies on the standard robustness parameter, i.e., the tolerable fraction of adversarial workers. Through theoretical analysis, we explained ARC's ability to enhance the robustness of Robust-DGD, particularly when the model is well-initialized. This phenomenon was validated through comprehensive experiments on standard image classification datasets. In short, our experiments showed that ARC consistently boosts the performance of Robust-DGD, especially in scenarios with high heterogeneity and large fraction of adversarial workers.

Future direction. Our work also reveals a gap between theory and practice in Byzantine machine learning (ML). While Robust-DGD and ARC-enhanced Robust-DGD share the same worst-case convergence guarantees, their empirical performances are drastically different. In fact, and unsurprisingly, Byzantine ML theory focuses on worst-case guarantees, which, although essential, may not fully capture the practical realities of many learning settings. In practice, we often operate under favorable conditions (e.g., well-initialized models), where worst-case guarantees have limited relevance. This gap opens the door for future work that prioritizes practically-driven research in Byzantine ML, under conditions that are realizable in real-world scenarios. It encourages the development of robust distributed learning methods, like ARC, that can take full advantage of favorable practical conditions, thereby yielding relevant theoretical guarantees and superior empirical performance.

REFERENCES

Pedro Abdalla and Nikita Zhivotovskiy. Covariance estimation: Optimal dimension-free guarantees for adversarial corruption and heavy tails. *Journal of the European Mathematical Society*, 2024.

Zeyuan Allen-Zhu, Faeze Ebrahimianghazani, Jerry Li, and Dan Alistarh. Byzantine-resilient non-convex stochastic gradient descent. In *International Conference on Learning Representations*, 2020.

Youssef Allouah, Sadegh Farhadkhani, Rachid Guerraoui, Nirupam Gupta, Rafael Pinot, and John Stephan. Fixing by mixing: A recipe for optimal byzantine ml under heterogeneity. In Francisco Ruiz, Jennifer Dy, and Jan-Willem van de Meent (eds.), *Proceedings of The 26th International Conference on Artificial Intelligence and Statistics*, volume 206 of *Proceedings of Machine Learning Research*, pp. 1232–1300. PMLR, 25–27 Apr 2023a. URL https://proceedings.mlr.press/v206/allouah23a.html.

Youssef Allouah, Rachid Guerraoui, Nirupam Gupta, Rafael Pinot, and Geovani Rizk. Robust distributed learning: Tight error bounds and breakdown point under data heterogeneity. In *Thirty-seventh Conference on Neural Information Processing Systems*, 2023b.

Gilad Baruch, Moran Baruch, and Yoav Goldberg. A little is enough: Circumventing defenses for distributed learning. In H. Wallach, H. Larochelle, A. Beygelzimer, F. d'Alché-Buc, E. Fox, and R. Garnett (eds.), *Advances in Neural Information Processing Systems*, volume 32. Curran Associates, Inc., 2019. URL https://proceedings.neurips.cc/paper_files/paper/2019/file/ec1c59141046cd1866bbbcdfb6ae31d4-Paper.pdf.

Peva Blanchard, El Mahdi El Mhamdi, Rachid Guerraoui, and Julien Stainer. Machine learning with adversaries: Byzantine tolerant gradient descent. In I. Guyon, U. V. Luxburg, S. Bengio, H. Wallach, R. Fergus, S. Vishwanathan, and R. Garnett (eds.), *Advances in Neural Information Processing Systems 30*, pp. 119–129. Curran Associates, Inc., 2017.

Léon Bottou, Frank E Curtis, and Jorge Nocedal. Optimization methods for large-scale machine learning. *Siam Review*, 60(2):223–311, 2018.

Stephen Boyd and Lieven Vandenberghe. *Convex optimization*. Cambridge university press, 2004.

Yudong Chen, Lili Su, and Jiaming Xu. Distributed statistical machine learning in adversarial settings: Byzantine gradient descent. *Proceedings of the ACM on Measurement and Analysis of Computing Systems*, 1(2):1–25, 2017.

M Danilova. Algorithms with gradient clipping for stochastic optimization with heavy-tailed noise. In *Doklady Mathematics*, volume 108, pp. S248–S256. Springer, 2023.

Li Deng. The mnist database of handwritten digit images for machine learning research. *IEEE Signal Processing Magazine*, 29(6):141–142, 2012.

Ilias Diakonikolas, Daniel M Kane, and Ankit Pensia. Outlier robust mean estimation with sub-gaussian rates via stability. *Advances in Neural Information Processing Systems*, 33:1830–1840, 2020.

Sadegh Farhadkhani, Rachid Guerraoui, Nirupam Gupta, Rafael Pinot, and John Stephan. Byzantine machine learning made easy by resilient averaging of momentums. In Kamalika Chaudhuri, Stefanie Jegelka, Le Song, Csaba Szepesvari, Gang Niu, and Sivan Sabato (eds.), *Proceedings of the 39th International Conference on Machine Learning*, volume 162 of *Proceedings of Machine Learning Research*, pp. 6246–6283. PMLR, 17–23 Jul 2022.

Sadegh Farhadkhani, Rachid Guerraoui, Nirupam Gupta, Lê-Nguyên Hoang, Rafael Pinot, and John Stephan. Robust collaborative learning with linear gradient overhead. In Andreas Krause, Emma Brunskill, Kyunghyun Cho, Barbara Engelhardt, Sivan Sabato, and Jonathan Scarlett (eds.), *Proceedings of the 40th International Conference on Machine Learning*, volume 202 of *Proceedings of Machine Learning Research*, pp. 9761–9813. PMLR, 23–29 Jul 2023. URL https://proceedings.mlr.press/v202/farhadkhani23a.html.

Xavier Glorot and Yoshua Bengio. Understanding the difficulty of training deep feedforward neural networks. In *Proceedings of the thirteenth international conference on artificial intelligence and statistics*, pp. 249–256. JMLR Workshop and Conference Proceedings, 2010.

Ian Goodfellow, Yoshua Bengio, and Aaron Courville. *Deep Learning*. MIT Press, 2016. http://www.deeplearningbook.org.

Eduard Gorbunov, Marina Danilova, and Alexander Gasnikov. Stochastic optimization with heavy-tailed noise via accelerated gradient clipping. *Advances in Neural Information Processing Systems*, 33:15042–15053, 2020.

Eduard Gorbunov, Marina Danilova, David Dobre, Pavel Dvurechenskii, Alexander Gasnikov, and Gauthier Gidel. Clipped stochastic methods for variational inequalities with heavy-tailed noise. *Advances in Neural Information Processing Systems*, 35:31319–31332, 2022.

Eduard Gorbunov, Samuel Horváth, Peter Richtárik, and Gauthier Gidel. Variance reduction is an antidote to byzantines: Better rates, weaker assumptions and communication compression as a cherry on the top. In *The Eleventh International Conference on Learning Representations*, 2023. URL https://openreview.net/forum?id=pfuqQQCB34.

Rachid Guerraoui, Nirupam Gupta, and Rafael Pinot. Byzantine machine learning: A primer. *ACM Computing Surveys*, 2023.

Nirupam Gupta and Nitin H Vaidya. Fault-tolerance in distributed optimization: The case of redundancy. In *Proceedings of the 39th Symposium on Principles of Distributed Computing*, pp. 365–374, 2020.

Kaiming He, Xiangyu Zhang, Shaoqing Ren, and Jian Sun. Deep residual learning for image recognition, 2015.

C. A. R. Hoare. Algorithm 65: Find. *Commun. ACM*, 4(7):321–322, jul 1961. ISSN 0001-0782. doi: 10.1145/366622.366647. URL https://doi.org/10.1145/366622.366647.

Tzu-Ming Harry Hsu, Hang Qi, and Matthew Brown. Measuring the effects of non-identical data distribution for federated visual classification, 2019a. URL https://arxiv.org/abs/1909.06335.

Tzu-Ming Harry Hsu, Hang Qi, and Matthew Brown. Measuring the effects of non-identical data distribution for federated visual classification, 2019b.

Peter Kairouz, H. Brendan McMahan, Brendan Avent, Aurélien Bellet, Mehdi Bennis, Arjun Nitin Bhagoji, Kallista Bonawitz, Zachary Charles, Graham Cormode, Rachel Cummings, Rafael G. L. D'Oliveira, Hubert Eichner, Salim El Rouayheb, David Evans, Josh Gardner, Zachary Garrett, Adrià Gascón, Badih Ghazi, Phillip B. Gibbons, Marco Gruteser, Zaid Harchaoui, Chaoyang He, Lie He, Zhouyuan Huo, Ben Hutchinson, Justin Hsu, Martin Jaggi, Tara Javidi, Gauri Joshi, Mikhail Khodak, Jakub Konecný, Aleksandra Korolova, Farinaz Koushanfar, Sanmi Koyejo, Tancrède Lepoint, Yang Liu, Prateek Mittal, Mehryar Mohri, Richard Nock, Ayfer Özgür, Rasmus Pagh, Hang Qi, Daniel Ramage, Ramesh Raskar, Mariana Raykova, Dawn Song, Weikang Song, Sebastian U. Stich, Ziteng Sun, Ananda Theertha Suresh, Florian Tramèr, Praneeth Vepakomma, Jianyu Wang, Li Xiong, Zheng Xu, Qiang Yang, Felix X. Yu, Han Yu, and Sen Zhao. Advances and open problems in federated learning. *Foundations and Trends® in Machine Learning*, 14(1–2): 1–210, 2021. ISSN 1935-8237. doi: 10.1561/2200000083.

Sai Praneeth Karimireddy, Satyen Kale, Mehryar Mohri, Sashank Reddi, Sebastian Stich, and Ananda Theertha Suresh. Scaffold: Stochastic controlled averaging for federated learning. In *International Conference on Machine Learning*, pp. 5132–5143. PMLR, 2020.

Sai Praneeth Karimireddy, Lie He, and Martin Jaggi. Learning from history for Byzantine robust optimization. *International Conference On Machine Learning, Vol 139*, 139, 2021.

Sai Praneeth Karimireddy, Lie He, and Martin Jaggi. Byzantine-robust learning on heterogeneous datasets via bucketing. In *International Conference on Learning Representations*, 2022. URL https://openreview.net/forum?id=jXKKDEi5vJt.

Sarit Khirirat, Eduard Gorbunov, Samuel Horváth, Rustem Islamov, Fakhri Karray, and Peter Richtárik. Clip21: Error feedback for gradient clipping. *arXiv preprint arXiv:2305.18929*, 2023.

Anastasia Koloskova, Hadrien Hendrikx, and Sebastian U. Stich. Revisiting gradient clipping: stochastic bias and tight convergence guarantees. In *Proceedings of the 40th International Conference on Machine Learning*, ICML'23. JMLR.org, 2023.

Alex Krizhevsky, Vinod Nair, and Geoffrey Hinton. The CIFAR-10 dataset. *online: http://www. cs. toronto. edu/kriz/cifar. html*, 55(5), 2014.

Leslie Lamport, Robert Shostak, and Marshall Pease. The Byzantine generals problem. *ACM Trans. Program. Lang. Syst.*, 4(3):382–401, jul 1982. ISSN 0164-0925. doi: 10.1145/357172.357176. URL https://doi.org/10.1145/357172.357176.

Shuo Liu, Nirupam Gupta, and Nitin H. Vaidya. Approximate Byzantine fault-tolerance in distributed optimization. In *Proceedings of the 2021 ACM Symposium on Principles of Distributed Computing*, PODC'21, pp. 379–389, New York, NY, USA, 2021. Association for Computing Machinery. ISBN 9781450385480. doi: 10.1145/3465084.3467902.

Guodong Long, Yue Tan, Jing Jiang, and Chengqi Zhang. Federated learning for open banking. In *Federated Learning: Privacy and Incentive*, pp. 240–254. Springer, 2020.

Grigory Malinovsky, Peter Richtárik, Samuel Horváth, and Eduard Gorbunov. Byzantine robustness and partial participation can be achieved simultaneously: Just clip gradient differences. *arXiv preprint arXiv:2311.14127*, 2023.

Brendan McMahan, Eider Moore, Daniel Ramage, Seth Hampson, and Blaise Aguera y Arcas. Communication-Efficient Learning of Deep Networks from Decentralized Data. In Aarti Singh and Jerry Zhu (eds.), *Proceedings of the 20th International Conference on Artificial Intelligence and Statistics*, volume 54 of *Proceedings of Machine Learning Research*, pp. 1273–1282. PMLR, 20–22 Apr 2017. URL https://proceedings.mlr.press/v54/mcmahan17a.html.

El Mahdi El Mhamdi, Rachid Guerraoui, and Sébastien Rouault. Distributed momentum for byzantine-resilient stochastic gradient descent. In *International Conference on Learning Representations*, 2021. URL https://openreview.net/forum?id=H8UHdhWG6A3.

Dinh C. Nguyen, Quoc-Viet Pham, Pubudu N. Pathirana, Ming Ding, Aruna Seneviratne, Zihuai Lin, Octavia Dobre, and Won-Joo Hwang. Federated learning for smart healthcare: A survey. *ACM Comput. Surv.*, 55(3), feb 2022. ISSN 0360-0300. doi: 10.1145/3501296. URL https://doi.org/10.1145/3501296.

Venkatadheeraj Pichapati, Ananda Theertha Suresh, Felix X. Yu, Sashank J. Reddi, and Sanjiv Kumar. Adaclip: Adaptive clipping for private SGD. *CoRR*, abs/1908.07643, 2019. URL http://arxiv.org/abs/1908.07643.

Lili Su and Nitin H Vaidya. Fault-tolerant multi-agent optimization: optimal iterative distributed algorithms. In *Proceedings of the 2016 ACM symposium on principles of distributed computing*, pp. 425–434, 2016.

Sharan Vaswani, Francis Bach, and Mark Schmidt. Fast and faster convergence of SGD for over-parameterized models and an accelerated perceptron. In *The 22nd international conference on artificial intelligence and statistics*, pp. 1195–1204. PMLR, 2019.

Han Xiao, Kashif Rasul, and Roland Vollgraf. Fashion-mnist: a novel image dataset for benchmarking machine learning algorithms. *arXiv preprint arXiv:1708.07747*, 2017.

Cong Xie, Oluwasanmi Koyejo, and Indranil Gupta. Fall of empires: Breaking byzantine-tolerant sgd by inner product manipulation. In Ryan P. Adams and Vibhav Gogate (eds.), *Proceedings of The 35th Uncertainty in Artificial Intelligence Conference*, volume 115 of *Proceedings of Machine Learning Research*, pp. 261–270. PMLR, 22–25 Jul 2020. URL https://proceedings.mlr.press/v115/xie20a.html.

Dong Yin, Yudong Chen, Ramchandran Kannan, and Peter Bartlett. Byzantine-robust distributed learning: Towards optimal statistical rates. In *International Conference on Machine Learning*, pp. 5650–5659. PMLR, 2018.

Bohang Zhang, Jikai Jin, Cong Fang, and Liwei Wang. Improved analysis of clipping algorithms for non-convex optimization. In *Proceedings of the 34th International Conference on Neural Information Processing Systems*, NIPS'20, Red Hook, NY, USA, 2020a. Curran Associates Inc. ISBN 9781713829546.

Jingzhao Zhang, Tianxing He, Suvrit Sra, and Ali Jadbabaie. Why gradient clipping accelerates training: A theoretical justification for adaptivity. In *International Conference on Learning Representations*, 2020b. URL `https://openreview.net/forum?id=BJgnXpVYwS`.

Xinwei Zhang, Xiangyi Chen, Mingyi Hong, Steven Wu, and Jinfeng Yi. Understanding clipping for federated learning: Convergence and client-level differential privacy. In *International Conference on Machine Learning*, pp. 26048–26067. PMLR, 2022.

A Computational Complexity of ARC.

The algorithm starts by computing the norms of all input vectors, which takes $\mathcal{O}(nd)$ time. Note that this step is also required for static clipping. The sorting operation of the norms takes $\mathcal{O}(n\log(n))$ time. Note that if n is large compared to $k = \lfloor 2(f/n)(n-f)\rfloor$, one can use more efficient algorithms for finding the $(k+1)$-th largest element, such as quick-select Hoare (1961) which has an average-case complexity of $\mathcal{O}(n)$. Finally, clipping the vectors requires $\mathcal{O}(nd)$ time. Therefore, the total complexity of ARC is $\mathcal{O}(nd + n\log(n))$. Overall, the complexity is comparable to static clipping, given that the sorting (or search) is crucially *dimension independent*.

B Proofs for Results in Section 3

Proofs for Lemma 3.1 and Theorem 3.2 are presented in B.1 and B.2, respectively.

Notation Let $n \in \mathbb{N}^*$. Given vectors $x_1, \ldots, x_n \in \mathbb{R}^d$ and a set $S \subseteq [n]$, we denote by $\overline{x}_S$ the mean of the vectors in S $\overline{x}_S = \frac{1}{|S|}\sum_{i\in S} x_i$. Given a clipping parameter $C \geq 0$, let

$$y_i \coloneqq \mathrm{clip}_C(x_i) = \min\left(1, \frac{C}{\|x_i\|}\right) x_i,$$

and

$$\overline{y}_S \coloneqq \frac{1}{|S|}\sum_{i\in S} y_i.$$

We denote by S_c the set of clipped vectors in S,

$$S_c \coloneqq \{i \in S, \|x_i\| > C\}. \tag{2}$$

Recall that we denote by $\mathbf{Clip}_C$ be the operator such that, for $x_1, \ldots, x_n \in \mathbb{R}^d$

$$\mathbf{Clip}_C(x_1, \ldots, x_n) \coloneqq (\mathrm{clip}_C(x_1), \ldots, \mathrm{clip}_C(x_n)) \ .$$

Further, let $\mathbf{F} : \mathbb{R}^{n\times d} \to \mathbb{R}^d$. We denote by $\mathbf{F} \circ \mathbf{Clip}_C$ the aggregation rule that first clips the input vectors using parameter C, and then aggregates them using $\mathbf{F}$

$$\mathbf{F} \circ \mathbf{Clip}_C(x_1, \ldots, x_n) \coloneqq \mathbf{F}(\mathbf{Clip}_C(x_1, \ldots, x_n)) \ .$$

B.1 Proof of Lemma 3.1

Lemma 3.1. *For any fixed $C \in \mathbb{R}^+$ and $\kappa' \geq 0$, $\mathbf{F} \circ \mathbf{Clip}_C$ is not (f, κ')-robust.*

Proof. We use reasoning by contradiction to prove the lemma.

We first consider the case when $C > 0$. Let $S \coloneqq \{1, \ldots, n-f\}$. Consider an arbitrary set of n vectors $x_1, \ldots, x_n$ in $\mathbb{R}^d$ such that $x_1 = \ldots = x_{n-f} = \overline{x}_S$ and $\|\overline{x}_S\| = 2C$. We assume that that $\mathbf{F} \circ \mathbf{Clip}_C$ is (f, κ')-robust for some $\kappa' \geq 0$. This assumption implies that

$$\|\mathbf{F} \circ \mathbf{Clip}_C(x_1, \ldots, x_n) - \overline{x}_S\|^2 \leq \frac{\kappa'}{|S|} \sum_{i \in S} \|x_i - \overline{x}_S\|^2 = 0. \tag{3}$$

Therefore,

$$\mathbf{F} \circ \mathbf{Clip}_C(x_1, \ldots, x_n) = \overline{x}_S.$$

However, the clipping operation results in $\mathrm{clip}_C(x_1) = \ldots = \mathrm{clip}_C(x_{n-f}) = \frac{1}{2}\overline{x}_S$. Therefore, by (f, κ)-robustness of $\mathbf{F}$,

$$\mathbf{F} \circ \mathbf{Clip}_C(x_1, \ldots, x_n) = \mathbf{F}\left(\frac{1}{2}\overline{x}_S, \ldots, \frac{1}{2}\overline{x}_S, \mathrm{clip}_C(x_{n-f+1}), \ldots, \mathrm{clip}_C(x_n)\right) = \frac{1}{2}\overline{x}_S.$$

This contradicts (3). As this contradiction holds for any value of κ', $\mathbf{F} \circ \mathbf{Clip}_C$ cannot be (f, κ')-robust for any κ'.

The proof for the case when $C = 0$ is similar to the above, where we choose $x_1 = \ldots = x_{n-f} = \overline{x}_S$ such that $\overline{x}_S$ is any vector with strictly positive norm. □

B.2 Proof of Theorem 3.2

Our proof relies on the following lemma, proof of which is deferred to B.2.1.

Lemma B.1. *Let $C \in \mathbb{R}^+$ and $\mathbf{F}$ be an (f, κ)-robust aggregation rule. Consider an arbitrary set of n vectors $x_1, x_2, \ldots, x_n \in \mathbb{R}^d$ and an arbitrary $S \subseteq [n]$ with $|S| = n - f$. Let S_c denote the set of indices of clipped vectors in S, i.e., $S_c \coloneqq \{i \in S, \|x_i\| > C\}$. If $|S \setminus S_c| \geq 1$, then*

$$\|\mathbf{F} \circ \mathbf{Clip}_C(x_1, \ldots, x_n) - \overline{x}_S\|^2 \leq \frac{\tilde{\kappa}}{|S|} \sum_{i \in S} \|x_i - \overline{x}_S\|^2 \quad ,$$

where $\tilde{\kappa} = \kappa + \frac{|S_c|}{|S \setminus S_c|}$.

Lemma B.1 shows that $\mathbf{F} \circ \mathbf{Clip}_C$ is $(f, \tilde{\kappa})$-robust, provided that $|S \setminus S_c| \geq 1$ for all subsets S of size $n - f$. Note that this condition is impossible to guarantee when using a fixed clipping threshold that does not depend on the input vectors. In order to ensure that $|S \setminus S_c| \geq 1$ for all subsets S of size $n - f$, the clipping threshold C should be large enough such that less than $n - f$ input vectors are clipped. By construction, ARC satisfies the condition of Lemma B.1. This brings us to the proof of Theorem 3.2, which we recall below for convenience.

Theorem 3.2. *If $\mathbf{F}$ is (f, κ)-robust, then $\mathbf{F} \circ \mathbf{ARC}$ is $\left(f, \kappa + \frac{2f}{n-2f}\right)$-robust.*

Proof. Since we clip the largest $\lfloor 2(f/n)(n-f) \rfloor$ gradients, for a given $S \subseteq [n]$ with $|S| = n - f$ we have

$$|S_c| \leq \lfloor 2(f/n)(n-f) \rfloor \leq 2(f/n)(n-f).$$

Therefore,

$$|S \setminus S_c| = |S| - |S_c| \geq (n-f) - \frac{2f}{n}(n-f) = (n-f)\frac{n-2f}{n}.$$

Since it is assumed that $f < n/2$, we have

$$|S \setminus S_c| > \left(n - \frac{n}{2}\right)\frac{n-n}{n} = 0.$$

Thus, the condition $|S \setminus S_c| \geq 1$ is always verified. Hence, from Lemma B.1 we obtain that $\mathbf{F} \circ \mathbf{ARC}$ is $\left(f, \left(\kappa + \frac{|S_c|}{|S \setminus S_c|}\right)\right)$-robust where

$$\frac{|S_c|}{|S \setminus S_c|} \leq \frac{2(f/n)(n-f)}{(n-f)\frac{n-2f}{n}} = \frac{2f}{n-2f}.$$

This concludes the proof. □

B.2.1 PROOF OF LEMMA B.1

We start by giving bounds on the **variance** (Lemma B.2) and the **bias** (Lemma B.3 and Lemma B.4) due to the clipping operation. We combine these bounds to prove the theorem.

VARIANCE REDUCTION DUE TO CLIPPING

We start by giving a bound on the variance of the clipped vectors. Recall from (2) that $S_c \coloneqq \{i \in S, \|x_i\| > C\}$.

Lemma B.2. *Let $C \geq 0$, $n > 0$ and $f < \frac{n}{2}$. For all $S \subseteq [n]$ with $|S| = n - f$, the following holds true:*

1. *If $\|\overline{x}_S\| \leq C$ then*

$$\frac{1}{|S|}\sum_{i\in S}\|y_i - \overline{y}_S\|^2 \leq \frac{1}{|S|}\sum_{i\in S}\|x_i - \overline{x}_S\|^2 - \frac{1}{|S|}\sum_{i\in S_c}(\|x_i\| - C)^2.$$

2. *If $\|\overline{x}_S\| > C$ then*

$$\frac{1}{|S|}\sum_{i\in S}\|y_i - \overline{y}_S\|^2 \leq \frac{1}{|S|}\sum_{i\in S}\|x_i - \overline{x}_S\|^2 - \frac{|S\setminus S_c|}{|S|}(\|\overline{x}_S\| - C)^2 - \frac{1}{|S|}\sum_{i\in S_c}(\|x_i\| - \|\overline{x}_S\|)^2.$$

Proof. Note that

$$\begin{aligned}
\frac{1}{|S|}\sum_{i\in S}\|y_i - \overline{y}_S\|^2 &= \frac{1}{|S|}\sum_{i\in S}\|y_i - \overline{x}_S + \overline{x}_S - \overline{y}_S\|^2 \\
&= \frac{1}{|S|}\sum_{i\in S}\Big(\|y_i - \overline{x}_S\|^2 + \|\overline{x}_S - \overline{y}_S\|^2 + 2\langle y_i - \overline{x}_S, \overline{x}_S - \overline{y}_S\rangle\Big) \\
&= \frac{1}{|S|}\sum_{i\in S}\|y_i - \overline{x}_S\|^2 + \|\overline{x}_S - \overline{y}_S\|^2 + 2\left\langle \underbrace{\frac{1}{|S|}\sum_{i\in S} y_i}_{\overline{y}_S} - \overline{x}_S,\, \overline{x}_S - \overline{y}_S\right\rangle \\
&= \frac{1}{|S|}\sum_{i\in S}\|y_i - \overline{x}_S\|^2 + \|\overline{x}_S - \overline{y}_S\|^2 - 2\left\langle \overline{x}_S - \overline{y}_S,\, \overline{x}_S - \overline{y}_S\right\rangle \\
&= \frac{1}{|S|}\sum_{i\in S}\|y_i - \overline{x}_S\|^2 - \|\overline{x}_S - \overline{y}_S\|^2 . \qquad (4)
\end{aligned}$$

By the definition of S_c (in (2)), for all $i \in S \setminus S_c$, $y_i = x_i$. Therefore,

$$\begin{aligned}
\frac{1}{|S|}\sum_{i\in S}\|y_i - \overline{x}_S\|^2 &= \frac{1}{|S|}\sum_{i\in S\setminus S_c}\|y_i - \overline{x}_S\|^2 + \frac{1}{|S|}\sum_{i\in S_c}\|y_i - \overline{x}_S\|^2 \\
&= \frac{1}{|S|}\sum_{i\in S\setminus S_c}\|x_i - \overline{x}_S\|^2 + \frac{1}{|S|}\sum_{i\in S_c}\|y_i - \overline{x}_S\|^2 .
\end{aligned}$$

The above can be written as

$$\frac{1}{|S|}\sum_{i\in S}\|y_i - \overline{x}_S\|^2 = \frac{1}{|S|}\sum_{i\in S}\|x_i - \overline{x}_S\|^2 + \frac{1}{|S|}\sum_{i\in S_c}(\|y_i - \overline{x}_S\|^2 - \|x_i - \overline{x}_S\|^2). \qquad (5)$$

For $i \in S_c$, we have $y_i = \frac{C}{\|x_i\|} x_i$. Thus, for all $i \in S_c$, we obtain that

$$\begin{aligned}
\|y_i - \overline{x}_S\|^2 - \|x_i - \overline{x}_S\|^2 &= \underbrace{\|y_i\|^2}_{=C^2} + \|\overline{x}_S\|^2 - 2\langle y_i, \overline{x}_S\rangle - \|x_i\|^2 - \|\overline{x}_S\|^2 + 2\langle x_i, \overline{x}_S\rangle \\
&= C^2 - \|x_i\|^2 + 2\left(1 - \frac{C}{\|x_i\|}\right)\langle x_i, \overline{x}_S\rangle \\
&= -(\|x_i\| - C)(\|x_i\| + C) + 2(\|x_i\| - C)\frac{\langle x_i, \overline{x}_S\rangle}{\|x_i\|} \\
&= (\|x_i\| - C)\left(2\frac{\langle x_i, \overline{x}_S\rangle}{\|x_i\|} - \|x_i\| - C\right).
\end{aligned}$$

By Cauchy-Schwarz inequality, we have $\langle x_i, \overline{x}_S\rangle \leq \|x_i\| \, \|\overline{x}_S\|$ Therefore,

$$\|y_i - \overline{x}_S\|^2 - \|x_i - \overline{x}_S\|^2 \leq (\|x_i\| - C)\left(2\|\overline{x}_S\| - \|x_i\| - C\right).$$

Substituting from the above in (5), we obtain that

$$\frac{1}{|S|}\sum_{i\in S}\|y_i - \overline{x}_S\|^2 \leq \frac{1}{|S|}\sum_{i\in S}\|x_i - \overline{x}_S\|^2 + \frac{1}{|S|}\sum_{i\in S_c}(\|x_i\| - C)\left(2\|\overline{x}_S\| - \|x_i\| - C\right).$$

Substituting from the above in (4), we obtain that

$$\frac{1}{|S|}\sum_{i\in S}\|y_i - \overline{y}_S\|^2 \leq \frac{1}{|S|}\sum_{i\in S}\|x_i - \overline{x}_S\|^2 + \frac{1}{|S|}\sum_{i\in S_c}(\|x_i\| - C)\left(2\|\overline{x}_S\| - \|x_i\| - C\right) - \|\overline{x}_S - \overline{y}_S\|^2. \tag{6}$$

We now consider below the two cases: $\|\overline{x}_S\| \leq C$ and $\|\overline{x}_S\| > C$.

In the first case, i.e,. when $\|\overline{x}_S\| \leq C$, we have

$$\begin{aligned}
\frac{1}{|S|}\sum_{i\in S_c}(\|x_i\| - C)\left(2\|\overline{x}_S\| - \|x_i\| - C\right) &\leq \frac{1}{|S|}\sum_{i\in S_c}(\|x_i\| - C)\left(2C - \|x_i\| - C\right) \\
&\leq -\frac{1}{|S|}\sum_{i\in S_c}(\|x_i\| - C)^2.
\end{aligned}$$

Substituting from the above in (6) yields the following

$$\begin{aligned}
\frac{1}{|S|}\sum_{i\in S}\|y_i - \overline{y}_S\|^2 &\leq \frac{1}{|S|}\sum_{i\in S}\|x_i - \overline{x}_S\|^2 - \frac{1}{|S|}\sum_{i\in S_c}(\|x_i\| - C)^2 - \|\overline{x}_S - \overline{y}_S\|^2 \\
&\leq \frac{1}{|S|}\sum_{i\in S}\|x_i - \overline{x}_S\|^2 - \frac{1}{|S|}\sum_{i\in S_c}(\|x_i\| - C)^2.
\end{aligned}$$

This proves the first part of the lemma.

Consider the second case, i.e., $\|\overline{x}_S\| > C$. Note that

$$\begin{aligned}
\frac{1}{|S|}\sum_{i\in S_c}(\|x_i\| - C)\left(2\|\overline{x}_S\| - \|x_i\| - C\right) &= \frac{1}{|S|}\sum_{i\in S_c}\left((\|\overline{x}_S\| - C)^2 - (\|x_i\| - \|\overline{x}_S\|)^2\right) \\
&= \frac{|S_c|}{|S|}(\|\overline{x}_S\| - C)^2 - \frac{1}{|S|}\sum_{i\in S_c}(\|x_i\| - \|\overline{x}_S\|)^2. \qquad (7)
\end{aligned}$$

Since $\|\overline{x}_S\| > C$, and $\|\overline{y}_S\| \leq C$, we have $\|\overline{x}_S\| - \|\overline{y}_S\| \geq \|\overline{x}_S\| - C \geq 0$. This, in conjunction with the reverse triangle inequality, implies that

$$\|\overline{x}_S - \overline{y}_S\|^2 \geq (\|\overline{x}_S\| - \|\overline{y}_S\|)^2 \geq (\|\overline{x}_S\| - C)^2. \tag{8}$$

Substituting from (7) and (8) in (6) yields the following:

$$\begin{aligned}\frac{1}{|S|}\sum_{i\in S}\|y_i-\overline{y}_S\|^2 &\leq \frac{1}{|S|}\sum_{i\in S}\|x_i-\overline{x}_S\|^2+\frac{|S_c|}{|S|}(\|\overline{x}_S\|-C)^2-\frac{1}{|S|}\sum_{i\in S_c}(\|x_i\|-\|\overline{x}_S\|)^2-(\|\overline{x}_S\|-C)^2\\ &\leq \frac{1}{|S|}\sum_{i\in S}\|x_i-\overline{x}_S\|^2+\left(\frac{|S_c|}{|S|}-1\right)(\|\overline{x}_S\|-C)^2-\frac{1}{|S|}\sum_{i\in S_c}(\|x_i\|-\|\overline{x}_S\|)^2\\ &= \frac{1}{|S|}\sum_{i\in S}\|x_i-\overline{x}_S\|^2-\frac{|S\setminus S_c|}{|S|}(\|\overline{x}_S\|-C)^2-\frac{1}{|S|}\sum_{i\in S_c}(\|x_i\|-\|\overline{x}_S\|)^2.\end{aligned}$$

This proves the second part, which concludes the proof of the lemma. □

BIAS DUE TO CLIPPING

We now bound the bias induced by clipping the input vectors.

Lemma B.3. *Let $C\geq 0$, $n>0$, $f<\frac{n}{2}$, and $S\subseteq[n]$, $|S|=n-f$. Then,*

$$\|\overline{x}_S-\overline{y}_S\|^2\leq\frac{|S_c|}{|S|^2}\sum_{i\in S_c}(\|x_i\|-C)^2.$$

Proof. Note that

$$\|\overline{x}_S-\overline{y}_S\|^2=\left\|\frac{1}{|S|}\sum_{i\in S}x_i-\frac{1}{|S|}\sum_{i\in S}y_i\right\|^2=\left\|\frac{1}{|S|}\sum_{i\in S}(x_i-y_i)\right\|^2.$$

As $x_i=y_i$ for all $i\in S\setminus S_c$, we have

$$\|\overline{x}_S-\overline{y}_S\|^2=\frac{1}{|S|^2}\left\|\sum_{i\in S_c}(x_i-y_i)\right\|^2.$$

Due to Jensen's inequality,

$$\|\overline{x}_S-\overline{y}_S\|^2=\frac{|S_c|^2}{|S|^2}\left\|\frac{1}{|S_c|}\sum_{i\in S_c}(x_i-y_i)\right\|^2\leq\frac{|S_c|}{|S|^2}\sum_{i\in S_c}\|x_i-y_i\|^2.$$

As $y_i=\frac{C}{\|x_i\|}x_i$ for all $i\in S_c$, substituting this in the above proves the lemma. □

We now show that the bias is upper bounded by a multiplicative factor of the variance of the input vectors, as long as there is at least one unclipped honest vector.

Lemma B.4 (Bias due to clipping)**.** *$C\geq 0$, $n>0$, $f<n/2$, and $S\subseteq[n]$, $|S|=n-f$, if $|S\setminus S_c|\geq 1$ then*

$$\|\overline{x}_S-\overline{y}_S\|^2\leq\frac{|S_c|}{|S\setminus S_c|}\frac{1}{|S|}\sum_{i\in S}\|x_i-\overline{x}_S\|^2.$$

Proof. We assume throughout the proof that $|S_c|>0$. Otherwise, if $|S_c|=0$, the bias is 0 and the statement is trivially true.

By Lemma B.3, we have

$$\|\overline{x}_S-\overline{y}_S\|^2\leq\frac{|S_c|}{|S|^2}\sum_{i\in S_c}(\|x_i\|-C)^2. \tag{9}$$

We distinguish two cases: $\|\overline{x}_S\|\leq C$ and $\|\overline{x}_S\|>C$. In the first case we have that

$$0\leq\|x_i\|-C\leq\|x_i\|-\|\overline{x}_S\|.$$

Substituting the above in (9), we find

$$\|\overline{x}_S - \overline{y}_S\|^2 \leq \frac{|S_c|}{|S|^2} \sum_{i \in S_c} (\|x_i\| - \|\overline{x}_S\|)^2 \leq \frac{|S_c|}{|S|^2} \sum_{i \in S} (\|x_i\| - \|\overline{x}_S\|)^2.$$

Using the reverse triangle inequality, we have that $(\|x_i\| - \|\overline{x}_S\|)^2 \leq \|x_i - \overline{x}_S\|^2$. This implies that

$$\|\overline{x}_S - \overline{y}_S\|^2 \leq \frac{|S_c|}{|S|^2} \sum_{i \in S} (\|x_i\| - \|\overline{x}_S\|)^2 \leq \frac{|S_c|}{|S \setminus S_c|} \frac{1}{|S|} \sum_{i \in S} \|x_i - \overline{x}_S\|^2 .$$

This proves the result for the first case.

Consider now the second case, i.e $\|\overline{x}_S\| > C$. Noting that we assume that $|S \setminus S_c| \geq 1$ and using Young's inequality with $c = \frac{|S_c|}{|S \setminus S_c|}$, we find, for any $i \in S_c$,

$$\begin{aligned}
(\|x_i\| - C)^2 &= (\|x_i\| - \|\overline{x}_S\| + \|\overline{x}_S\| - C)^2 \\
&\leq (1 + c)(\|x_i\| - \|\overline{x}_S\|)^2 + (1 + 1/c)(\|\overline{x}_S\| - C)^2) \\
&= \frac{|S_c| + |S \setminus S_c|}{|S \setminus S_c|} (\|x_i\| - \|\overline{x}_S\|)^2 + \frac{|S_c| + |S \setminus S_c|}{|S_c|} (\|\overline{x}_S\| - C)^2.
\end{aligned}$$

Recall from (2) that $S_c \coloneqq \{i \in S, \|x_i\| > C\}$. This implies that $|S_c| + |S \setminus S_c| = |S|$. Therefore

$$(\|x_i\| - C)^2 \leq |S| \left(\frac{1}{|S \setminus S_c|} (\|x_i\| - \|\overline{x}_S\|)^2 + \frac{1}{|S_c|} (\|\overline{x}_S\| - C)^2 \right). \tag{10}$$

Substituting (10) in (9), we find

$$\begin{aligned}
\|\overline{x}_S - \overline{y}_S\|^2 &\leq \frac{|S_c|}{|S|^2} \sum_{i \in S_c} |S| \left(\frac{1}{|S \setminus S_c|} (\|x_i\| - \|\overline{x}_S\|)^2 + \frac{1}{|S_c|} (\|\overline{x}_S\| - C)^2 \right) \\
&= \frac{|S_c|}{|S|} \left(\frac{1}{|S \setminus S_c|} \sum_{i \in S_c} (\|x_i\| - \|\overline{x}_S\|)^2 + (\|\overline{x}_S\| - C)^2 \right). \qquad (11)
\end{aligned}$$

Since $\|\overline{x}_S\| > C$, we have for any $i \in S \setminus S_c$

$$0 \leq \|\overline{x}_S\| - C \leq \|\overline{x}_S\| - \|x_i\| .$$

Therefore

$$|S \setminus S_c| \, (\|\overline{x}_S\| - C)^2 \leq \sum_{i \in S \setminus S_c} (\|\overline{x}_S\| - \|x_i\|)^2$$

Which gives the bound

$$(\|\overline{x}_S\| - C)^2 \leq \frac{1}{|S \setminus S_c|} \sum_{i \in S \setminus S_c} (\|\overline{x}_S\| - \|x_i\|)^2. \tag{12}$$

Substituting (12) in (11), we find

$$\begin{aligned}
\|\overline{x}_S - \overline{y}_S\|^2 &\leq \frac{|S_c|}{|S|} \left(\frac{1}{|S \setminus S_c|} \sum_{i \in S_c} (\|x_i\| - \|\overline{x}_S\|)^2 + \frac{1}{|S \setminus S_c|} \sum_{i \in S \setminus S_c} (\|x_i\| - \|\overline{x}_S\|)^2 \right) \\
&= \frac{|S_c|}{|S \setminus S_c|} \frac{1}{|S|} \sum_{i \in S} (\|x_i\| - \|\overline{x}_S\|)^2 \leq \frac{|S_c|}{|S \setminus S_c|} \frac{1}{|S|} \sum_{i \in S} \|x_i - \overline{x}_S\|^2 .
\end{aligned}$$

This proves the result for the second case and concludes the proof. □

PROOF OF LEMMA B.1

Let us recall the lemma below.

Lemma B.1. *Let $C \in \mathbb{R}^+$ and $\mathbf{F}$ be an (f, κ)-robust aggregation rule. Consider an arbitrary set of n vectors $x_1, x_2, \ldots, x_n \in \mathbb{R}^d$ and an arbitrary $S \subseteq [n]$ with $|S| = n - f$. Let S_c denote the set of indices of clipped vectors in S, i.e., $S_c \coloneqq \{i \in S, \|x_i\| > C\}$. If $|S \setminus S_c| \geq 1$, then*

$$\|\mathbf{F} \circ \mathbf{Clip}_C(x_1, \ldots, x_n) - \overline{x}_S\|^2 \leq \frac{\tilde{\kappa}}{|S|} \sum_{i \in S} \|x_i - \overline{x}_S\|^2 \quad ,$$

where $\tilde{\kappa} = \kappa + \frac{|S_c|}{|S \setminus S_c|}$.

Proof. We assume throughout the proof that $|S_c| > 0$. Otherwise, the statement is trivially true by (f, κ)-robustness of $\mathbf{F}$ and the fact that the vectors in S remain unchanged after the clipping operation.

Consider first the case $\kappa = 0$. Since $\kappa \geq \frac{f}{n-2f}$ [5], we have that $f = 0$. Recall that we denote $y_i \coloneqq \mathrm{clip}_C(x_i)$ and $\overline{y}_S \coloneqq \frac{1}{|S|} \sum_{i \in S} y_i$. Since $\kappa = 0$, the output of $\mathbf{F}$ will correspond to the average of its input, which implies that

$$\|\mathbf{F} \circ \mathbf{Clip}_C(x_1, \ldots, x_n) - \overline{y}_S\|^2 = \|\mathbf{F}(y_1, \ldots, y_n) - \overline{y}_S\|^2 = 0.$$

Therefore

$$\mathbf{F} \circ \mathbf{Clip}_C(x_1, \ldots, x_n) = \overline{y}_S.$$

We find then

$$\|\mathbf{F} \circ \mathbf{Clip}_C(x_1, \ldots, x_n) - \overline{x}_S\|^2 = \|\overline{y}_S - \overline{x}_S\|^2 .$$

The result for the case $\kappa = 0$ follows from lemma B.4.

Suppose now that $\kappa > 0$. Using Young's inequality with $c = \frac{|S_c|}{\kappa |S \setminus S_c|}$ we find

$$\begin{aligned}\|\mathbf{F} \circ \mathbf{Clip}_C(x_1, \ldots, x_n) - \overline{x}_S\|^2 &= \|\mathbf{F} \circ \mathbf{Clip}_C(x_1, \ldots, x_n) - \overline{y}_S + \overline{y}_S - \overline{x}_S\|^2 \\ &\leq (1 + c) \|\mathbf{F} \circ \mathbf{Clip}_C(x_1, \ldots, x_n) - \overline{y}_S\|^2 + \left(1 + \frac{1}{c}\right) \|\overline{x}_S - \overline{y}_S\|^2 .\end{aligned} \tag{13}$$

On the one hand, by (f, κ)-robustness of $\mathbf{F}$, we have

$$\begin{aligned}(1 + c) \|\mathbf{F} \circ \mathbf{Clip}_C(x_1, \ldots, x_n) - \overline{y}_S\|^2 &= (1 + c) \|\mathbf{F}(y_1, \ldots, y_n) - \overline{y}_S\|^2 \\ &\leq (1 + c) \frac{\kappa}{|S|} \sum_{i \in S} \|y_i - \overline{y}_S\|^2 \\ &= \left(\kappa + \frac{|S_c|}{|S \setminus S_c|}\right) \frac{1}{|S|} \sum_{i \in S} \|y_i - \overline{y}_S\|^2 .\end{aligned} \tag{14}$$

On the other hand, we have

$$(1 + 1/c) \|\overline{x}_S - \overline{y}_S\|^2 = \left(1 + \frac{\kappa |S \setminus S_c|}{|S_c|}\right) \|\overline{x}_S - \overline{y}_S\|^2 = \left(\kappa + \frac{|S_c|}{|S \setminus S_c|}\right) \frac{|S \setminus S_c|}{|S_c|} \|\overline{x}_S - \overline{y}_S\|^2 . \tag{15}$$

Substituting (14) and (15) in (13) we obtain that

$$\|\mathbf{F} \circ \mathbf{Clip}_C(x_1, \ldots, x_n) - \overline{x}_S\|^2 \leq \left(\kappa + \frac{|S_c|}{|S \setminus S_c|}\right) \left(\frac{1}{|S|} \sum_{i \in S} \|y_i - \overline{y}_S\|^2 + \frac{|S \setminus S_c|}{|S_c|} \|\overline{x}_S - \overline{y}_S\|^2\right). \tag{16}$$

[5] Proposition 6, Allouah et al. (2023a)

We consider below the two cases $\|\overline{x}_S\| \leq C$ and $\|\overline{x}_S\| > C$ separately.

In the first case, we use the the first part of lemma B.2 and lemma B.3 to obtain that

$$\begin{aligned}
&\frac{1}{|S|}\sum_{i\in S}\|y_i - \overline{y}_S\|^2 + \frac{|S\setminus S_c|}{|S|}\|\overline{x}_S - \overline{y}_S\|^2 \\
&\leq \frac{1}{|S|}\sum_{i\in S}\|x_i - \overline{x}_S\|^2 - \frac{1}{|S|}\sum_{i\in S_c}(\|x_i\| - C)^2 + \frac{|S\setminus S_c|}{|S|}\frac{1}{|S|}\sum_{i\in S_c}(\|x_i\| - C)^2 \\
&= \frac{1}{|S|}\sum_{i\in S}\|x_i - \overline{x}_S\|^2 - \frac{|S_c|}{|S|}\frac{1}{|S|}\sum_{i\in S}(\|x_i\| - C)^2 \leq \frac{1}{|S|}\sum_{i\in S}\|x_i - \overline{x}_S\|^2 .
\end{aligned}$$

This proves the result for this case.

Consider the second case, i.e $\|\overline{x}_S\| > C$. Following the proof of corollary B.4 until (11) we have

$$\|\overline{x}_S - \overline{y}_S\|^2 \leq \frac{|S_c|}{|S|}\left(\frac{1}{|S\setminus S_c|}\sum_{i\in S_c}(\|x_i\| - \|\overline{x}_S\|)^2 + (\|\overline{x}_S\| - C)^2\right).$$

Therefore,

$$\begin{aligned}
\frac{|S\setminus S_c|}{|S_c|}\|\overline{x}_S - \overline{y}_S\|^2 &\leq \frac{|S\setminus S_c|}{|S|}\left(\frac{1}{|S\setminus S_c|}\sum_{i\in S_c}(\|x_i\| - \|\overline{x}_S\|)^2 + (\|\overline{x}_S\| - C)^2\right) \\
&\leq \frac{1}{|S|}\sum_{i\in S_c}(\|x_i\| - \|\overline{x}_S\|)^2 + \frac{|S\setminus S_c|}{|S|}(\|\overline{x}_S\| - C)^2.
\end{aligned}$$

Using the above in conjunction with lemma B.2 for the case $\|\overline{x}_S\| > C$ in (16) proves the result for the second case, which concludes the proof. □

C Proofs of the Results in Section 5

In this section, we first prove the *Bounded Aggregation Output* property of ARC in Lemma 5.1, and show that the other SOTA aggregation rules do not satisfy it in Lemma C.1. Then, to prove Theorem 5.2, we first prove Lemma C.2. We assume throughout this appendix that for any set of vectors $x_1, \ldots, x_n \in \mathbb{R}^d$, $\|\mathbf{F}(x_1, \ldots, x_n)\| \leq \max_{i\in[n]}\|x_i\|$. This assumption can be made without loss of generality, see Appendix C.1.

Lemma 5.1 (**Bounded Aggregation Output**). *Let* $\mathbf{F}$ *be an* (f, κ)*-robust aggregation method. For any vectors* $x_1, \ldots, x_n \in \mathbb{R}^d$ *and set* $S \subset [n]$ *such that* $|S| = n - f$*, the following holds true:*

$$\|\mathbf{F} \circ \mathbf{ARC}(x_1, \ldots, x_n)\| \leq \max_{i\in S}\|x_i\| \tag{1}$$

Proof. Without loss of generality and for the sake of simplicity, let us suppose that the vectors $x_1, \ldots, x_n$ are indexed such that $\|x_1\| \geq \|x_2\| \geq \cdots \geq \|x_n\|$. Let $(\tilde{x}_1, \ldots, \tilde{x}_n) = ARC(x_1, \ldots, x_n)$ be the clipped version of these vectors after applying ARC.

Case 1: When $f = 0$, $S = [n]$ and we clip all the vectors by $\|x_1\| = \max_{i\in S}\|x_i\|$, hence for any j, $\|\tilde{x}_j\| \leq \max_{i\in S}\|x_i\|$. Using the fact that for any set of vectors $x_1, \ldots, x_n \in \mathbb{R}^d$, $\|\mathbf{F}(x_1, \ldots, x_n)\| \leq \max_{i\in[n]}\|x_i\|$, we have

$$\|\mathbf{F} \circ ARC(x_1, \ldots, x_n)\| = \|\mathbf{F}(\tilde{x}_1, \ldots, \tilde{x}_n)\| \leq \max_{j\in[n]}\|\tilde{x}_j\| \leq \max_{i\in S}\|x_i\| \quad . \tag{17}$$

Case 2: When $0 < f < \frac{n}{2}$, as presented in Algorithm 2, ARC clips all the vectors $x_1, \ldots, x_n$ to $\|x_{k+1}\|$ where $k = \lfloor 2\frac{f}{n}(n - f)\rfloor$. Hence, for any $j \in [n]$,

$$\|\tilde{x}_j\| \leq \|x_{k+1}\| \quad . \tag{18}$$

We have that $k+1 = \lfloor 2\frac{f}{n}(n-f) \rfloor + 1 \geq 2\frac{f}{n}(n-f)$.

One can show that

$$\begin{aligned} \frac{2f}{n}(n-f) - f &= f(1 - \frac{2f}{n}) \\ &> 0, \quad \forall f \in \left]0, \frac{n}{2}\right[\end{aligned} \tag{19}$$

Hence, $\frac{2f}{n}(n-f) > f$, which gives $k+1 > f$, and since $k+1$ is an integer, we have $k+1 \geq f+1$. Hence we know that at least $f+1$ vectors have their norm greater or equal to the clipping threshold $C = \|x_{k+1}\|$,

$$\underbrace{\|x_1\| \leq \cdots \leq \|x_{k+1}\|}_{\text{at least } f+1 \text{ vectors}} \leq \underbrace{\|x_{k+2}\| \leq \cdots \leq \|x_n\|}_{\text{at most } n-f-1 \text{ vectors}}$$

Hence, at most $n-f-1$ vectors will not be clipped. For any subset of $S \subset [n]$ of size $n-f$, at least one of the vectors has its norm equal to the clipping threshold (i.e. $\max_{i \in S} \|x_i\| = \|x_{k+1}\|$) or will be clipped (i.e. $\max_{i \in S} \|x_i\| > \|x_{k+1}\|$). Hence, we have that

$$\max_{i \in S} \|x_i\| \geq \|x_{k+1}\| \quad . \tag{20}$$

Combining (18) and (20), we have that for all $j \in [n]$,

$$\|\tilde{x}_j\| \leq \max_{i \in S} \|x_i\| \quad .$$

Using the fact that for any set of vectors $x_1, \ldots, x_n \in \mathbb{R}^d$, $\|\mathbf{F}(x_1, \ldots, x_n)\| \leq \max_{i \in [n]} \|x_i\|$, we have

$$\|\mathbf{F} \circ ARC(x_1, \ldots, x_n)\| = \|\mathbf{F}(\tilde{x}_1, \ldots, \tilde{x}_n)\| \leq \max_{j \in [n]} \|\tilde{x}_j\| \leq \max_{i \in S} \|x_i\| \quad . \tag{21}$$

□

Lemma C.1. *For any aggregation rule* $\mathbf{F} \in \{\mathbf{CWTM}, \mathbf{CWMed}, \mathbf{GM}, \mathbf{MK}, \mathbf{CWTM} \circ \mathbf{NNM}, \mathbf{CWMed} \circ \mathbf{NNM}, \mathbf{GM} \circ \mathbf{NNM}, \mathbf{MK} \circ \mathbf{NNM}\}$*, there exists* $f \in [0, \frac{n}{2})$*, a set of vectors* $x_1, \ldots, x_n$ *and a subset* $S \subset [n]$*,* $|S| = n-f$ *such that*

$$\mathbf{F}(x_1, \ldots, x_n) \not\leq \max_{i \in S} \|x_i\| \tag{22}$$

Proof. Let us consider $(x_1, x_2, x_3) = ((0,1), (1,0), (1,1))$, and $S = \{x_1, x_2\}$,

For $\mathbf{F} \in \{\mathbf{CWTM}, \mathbf{CWMed}, \mathbf{GM}\}$, we have $\|\mathbf{F}(x_1, x_2, x_3)\| = \|(1,1)\| = \sqrt{2} > \max_{i \in S} \|x_i\| = \|x_1\| = 1$.

For $\mathbf{F} \in \{\mathbf{MK}, \mathbf{CWTM} \circ \mathbf{NNM}, \mathbf{CWMed} \circ \mathbf{NNM}, \mathbf{GM} \circ \mathbf{NNM}, \mathbf{MK} \circ \mathbf{NNM}\}$, we have $\|\mathbf{F}(x_1, x_2, x_3)\| = \|(0.5, 1)\| = \sqrt{1.25} > \max_{i \in S} \|x_i\| = \|x_1\| = 1$. □

Lemma C.2. *Let* $\mathbf{F}$ *be* (f, κ)*-robust. Let* Δ_o *and* ρ *be real values such that* $\mathcal{L}_{\mathcal{H}}(\theta_1) - \mathcal{L}^*_{\mathcal{H}} \leq \Delta_o$ *and* $\max_{i \in \mathcal{H}} \|\nabla \mathcal{L}_i(\theta_1)\| \leq \exp\left(-\frac{\Delta_o}{\kappa G^2} L\right) \rho$*. If* $\gamma = \min\left\{\left(\frac{\Delta_o}{\kappa G^2}\right)\frac{1}{T}, \frac{1}{L}\right\}$*, then*

$$\frac{1}{T} \sum_{t=1}^{T} \|\nabla \mathcal{L}_{\mathcal{H}}(\theta_t)\|^2 \leq \frac{2\Delta_o L}{T} + 5\kappa\left(G^2 + B^2\rho^2\right).$$

Our proof for Lemma C.2 relies on the following sub-result.

Lemma C.3. *For all* $t \in [T]$*, we obtain that*

$$\max_{i \in \mathcal{H}} \|\nabla \mathcal{L}_i(\theta_t)\| \leq \exp(\gamma L T) \max_{i \in \mathcal{H}} \|\nabla \mathcal{L}_i(\theta_1)\|.$$

Proof. Consider an arbitrary $t \in [T]$. Let $(x_1, \ldots, x_n) \coloneqq \mathbf{ARC}\left(g_t^{(1)}, \ldots, g_t^{(n)}\right)$. As $n > 2f$ and $|\mathcal{H}| = n - f$, the clipping threshold C used in ARC (see Algorithm 2) is bounded by $\max_{i \in \mathcal{H}} \left\|g_t^{(i)}\right\|$ (see (20) in Lemma 5.1). Therefore,

$$\max_{i \in [n]} \|x_i\| \leq \max_{i \in \mathcal{H}} \left\|g_t^{(i)}\right\| = \max_{i \in \mathcal{H}} \|\nabla \mathcal{L}_i(\theta_t)\| . \tag{23}$$

Since for any set of n vectors $z_1, \ldots, z_n \in \mathbb{R}^d$, $\|\mathbf{F}(z_1, \ldots, z_n)\| \leq \max_{i \in [n]} \|z_i\|$, from (23) we obtain that

$$\|R_t\| = \left\|\mathbf{F} \circ \mathbf{ARC}\left(g_t^{(1)}, \ldots, g_t^{(n)}\right)\right\| \leq \max_{i \in [n]} \|x_i\| \leq \max_{i \in \mathcal{H}} \|\nabla \mathcal{L}_i(\theta_t)\| .$$

Recall that $\theta_{t+1} \coloneqq \theta_t - \gamma R_t$. Thus, from above we obtain that

$$\left\|\theta_{t+1} - \theta_t\right\| \leq \gamma \max_{i \in \mathcal{H}} \|\nabla \mathcal{L}_i(\theta_t)\| . \tag{24}$$

Due to L-Lipschitz smoothness of $\mathcal{L}_i(\theta)$ for all $i \in \mathcal{H}$, the above implies that

$$\left\|\nabla \mathcal{L}_i(\theta_{t+1}) - \nabla \mathcal{L}_i(\theta_t)\right\| \leq \gamma L \max_{i \in \mathcal{H}} \|\nabla \mathcal{L}_i(\theta_t)\| , \quad \forall i \in \mathcal{H}.$$

This, in conjunction with the triangle inequality, implies that

$$\left\|\nabla \mathcal{L}_i(\theta_{t+1})\right\| \leq \|\nabla \mathcal{L}_i(\theta_t)\| + \gamma L \max_{i \in \mathcal{H}} \|\nabla \mathcal{L}_i(\theta_t)\| , \quad \forall i \in \mathcal{H}.$$

Therefore,

$$\max_{i \in \mathcal{H}} \left\|\nabla \mathcal{L}_i(\theta_{t+1})\right\| \leq \max_{i \in \mathcal{H}} \|\nabla \mathcal{L}_i(\theta_t)\| + \gamma L \max_{i \in \mathcal{H}} \|\nabla \mathcal{L}_i(\theta_t)\| = (1 + \gamma L) \max_{i \in \mathcal{H}} \|\nabla \mathcal{L}_i(\theta_t)\| .$$

As t was chosen arbitrarily from $[T]$, the above holds true for all $t \in [T]$. For an arbitrary $\tau \in [T]$, using the inequality recursively for $t = \tau, \ldots, 1$ we obtain that

$$\max_{i \in \mathcal{H}} \left\|\nabla \mathcal{L}_i(\theta_{\tau+1})\right\| \leq (1 + \gamma L)^{\tau} \max_{i \in \mathcal{H}} \|\nabla \mathcal{L}_i(\theta_1)\| \leq (1 + \gamma L)^{T} \max_{i \in \mathcal{H}} \|\nabla \mathcal{L}_i(\theta_1)\| .$$

Since $(1 + \gamma L)^T \leq \exp(\gamma L T)$, the above concludes the proof. □

We are now ready to present our **proof of Lemma C.2**.

Proof of Lemma C.2. For simplicity, we write $\mathcal{L}_{\mathcal{H}}$ as $\mathcal{L}$ throughout the proof.

Consider an arbitrary $t \in [T]$. Due to L-Lipschitz smoothness of $\mathcal{L}(\theta)$, we obtain that

$$\mathcal{L}(\theta_{t+1}) \leq \mathcal{L}(\theta_t) + \left\langle \theta_{t+1} - \theta_t, \nabla \mathcal{L}(\theta_t) \right\rangle + \frac{L}{2} \left\|\theta_{t+1} - \theta_t\right\|^2 .$$

Substituting $\theta_{t+1} = \theta_t - \gamma R_t$, and using the identity: $2 \langle a, b \rangle = \|a\|^2 + \|b\|^2 - \|a - b\|^2$, we obtain that

$$\mathcal{L}(\theta_{t+1}) \leq \mathcal{L}(\theta_t) - \frac{\gamma}{2} \|\nabla \mathcal{L}(\theta_t)\|^2 + \frac{\gamma}{2} \|R_t - \nabla \mathcal{L}(\theta_t)\|^2 - \frac{\gamma}{2} (1 - \gamma L) \|R_t\|^2 .$$

Since $\gamma \leq \frac{1}{L}$, $(1 - \gamma L) \geq 0$. Therefore, from above we obtain that

$$\mathcal{L}(\theta_{t+1}) \leq \mathcal{L}(\theta_t) - \frac{\gamma}{2} \|\nabla \mathcal{L}(\theta_t)\|^2 + \frac{\gamma}{2} \|R_t - \nabla \mathcal{L}(\theta_t)\|^2 .$$

Recall that t is chosen arbitrarily from $[T]$. Thus, the above holds true for all $t \in [T]$. Taking summation on both sides from $t = 1$ to $t = T$ we obtain that

$$\frac{\gamma}{2} \sum_{t=1}^{T} \|\nabla \mathcal{L}(\theta_t)\|^2 \leq \mathcal{L}(\theta_t) - \mathcal{L}(\theta_{T+1}) + \frac{\gamma}{2} \sum_{t=1}^{T} \|R_t - \nabla \mathcal{L}(\theta_t)\|^2 .$$

Multiplying both sides by $2/(\gamma T)$ we obtain that

$$\frac{1}{T}\sum_{t=1}^{T}\|\nabla\mathcal{L}(\theta_t)\|^2 \leq \frac{2\left(\mathcal{L}(\theta_1)-\mathcal{L}(\theta_{T+1})\right)}{\gamma T} + \frac{1}{T}\sum_{t=1}^{T}\|R_t-\nabla\mathcal{L}(\theta_t)\|^2.$$

Note that $\mathcal{L}(\theta_1)-\mathcal{L}(\theta_{T+1}) = \mathcal{L}(\theta_1)-\mathcal{L}^* - \left(\mathcal{L}(\theta_{T+1})-\mathcal{L}^*\right) \leq \mathcal{L}(\theta_1)-\mathcal{L}^* \leq \Delta_o$. Using this above we obtain that

$$\frac{1}{T}\sum_{t=1}^{T}\|\nabla\mathcal{L}(\theta_t)\|^2 \leq \frac{2\Delta_o}{\gamma T} + \frac{1}{T}\sum_{t=1}^{T}\|R_t-\nabla\mathcal{L}(\theta_t)\|^2.$$

Recall, by Theorem 3.2, that $\mathbf{F}\circ\mathbf{ARC}$ is $(f,3\kappa)$-robust. Therefore, by Definition 2.4, $\|R_t-\nabla\mathcal{L}(\theta_t)\|^2 \leq \frac{3\kappa}{|\mathcal{H}|}\sum_{i\in\mathcal{H}}\|\nabla\mathcal{L}_i(\theta_t)-\nabla\mathcal{L}(\theta_t)\|^2$ for all t. Using this above we obtain that

$$\frac{1}{T}\sum_{t=1}^{T}\|\nabla\mathcal{L}(\theta_t)\|^2 \leq \frac{2\Delta_o}{\gamma T} + \frac{3\kappa}{T}\sum_{t=1}^{T}\frac{1}{|\mathcal{H}|}\|\nabla\mathcal{L}_i(\theta_t)-\nabla\mathcal{L}(\theta_t)\|^2. \tag{25}$$

Note that, since $\gamma \leq \frac{\Delta_o}{\kappa G^2 T}$ and $\|\nabla\mathcal{L}_i(\theta_1)\| \leq \exp\left(-\frac{\Delta_o L}{\kappa G^2}\right)\rho$, by Lemma C.3 we have

$$\max_{i\in\mathcal{H}}\|\nabla\mathcal{L}_i(\theta_t)\| \leq \exp\left(\frac{\Delta_o L}{\kappa G^2}\right)\max_{i\in\mathcal{H}}\|\nabla\mathcal{L}_i(\theta_1)\| \leq \rho, \quad \forall t\in[T].$$

This, in conjunction with triangle inequality, implies that

$$\|\nabla\mathcal{L}(\theta_t)\| \leq \frac{1}{|\mathcal{H}|}\sum_{i\in\mathcal{H}}\|\nabla\mathcal{L}_i(\theta_t)\| \leq \rho, \quad \forall t\in[T].$$

Therefore, under (G,B)-gradient dissimilarity, for all $t\in[T]$,

$$\frac{1}{|\mathcal{H}|}\|\nabla\mathcal{L}_i(\theta_t)-\nabla\mathcal{L}(\theta_t)\|^2 \leq G^2 + B^2\,\rho^2.$$

Using this in (25) we obtain that

$$\frac{1}{T}\sum_{t=1}^{T}\|\nabla\mathcal{L}(\theta_t)\|^2 \leq \frac{2\Delta_o}{\gamma T} + 3\kappa\left(G^2+B^2\rho^2\right). \tag{26}$$

Consider the two cases: (i) $T \geq \frac{\Delta_o L}{\kappa G^2}$ and (ii) $T < \frac{\Delta_o L}{\kappa G^2}$. In case (i), $\gamma = \frac{\Delta_o}{\kappa G^2 T}$. Using this in (26) implies that

$$\frac{1}{T}\sum_{t=1}^{T}\|\nabla\mathcal{L}(\theta_t)\|^2 \leq 2\kappa G^2 + 3\kappa\left(G^2+B^2\rho^2\right) \leq 5\kappa\left(G^2+B^2\rho^2\right). \tag{27}$$

In case (ii), $\gamma = \frac{1}{L}$. Using this in (26) implies that

$$\frac{1}{T}\sum_{t=1}^{T}\|\nabla\mathcal{L}(\theta_t)\|^2 \leq \frac{2\Delta_o L}{T} + 3\kappa\left(G^2+B^2\rho^2\right). \tag{28}$$

Combining (27) and (28) concludes the proof. □

We now prove Theorem C.4, stated below, which immediately implies Theorem 5.2. Specifically, **Theorem 5.2 follows immediately from Part 1 of Theorem C.4, upon substituting $\xi \leq \frac{1}{\Psi(G,B,\rho)}\upsilon$.**

Theorem C.4. *Suppose $B>0$ and there exists $\zeta\in\mathbb{R}^+$ such that $\max_{i\in\mathcal{H}}\|\nabla\mathcal{L}_i(\theta_1)\| \leq \zeta$. Let $\mathbf{F}\in\{\mathbf{CWTM},\mathbf{CWMed},\mathbf{GM},\mathbf{MK}\}$, $\gamma = \min\left\{\left(\frac{\Delta_o}{\kappa G^2}\right)\frac{1}{T}, \frac{1}{L}\right\}$ and $T \geq \frac{\Delta_o L}{\kappa G^2}$. Consider an arbitrary real value $\xi_o\in(0,1)$. Let $\rho \coloneqq \exp\left(\frac{(2+B^2)\Delta_o}{(1-\xi_o)G^2}L\right)\zeta$. Then, the following holds true:*

1. *If $\frac{f}{n} \coloneqq (1-\xi)\mathsf{BP}$, where $\xi\in(0,\xi_o]$, then, $\mathbb{E}\left[\left\|\nabla\mathcal{L}_{\mathcal{H}}\left(\hat{\theta}\right)\right\|^2\right] \leq \xi\,\Psi(G,B,\rho)\,\varepsilon_o$.*

2. *If* $\mathsf{BP} \leq f/n < 1/2$*, then* $\mathbb{E}\left[\left\|\nabla \mathcal{L}_{\mathcal{H}}\left(\hat{\theta}\right)\right\|^2\right] \leq \Psi(G, B, \rho) \cdot \frac{G^2}{8}$.

In order to prove Theorem C.4, we first obtain the following corollary of Lemma C.2 and Lemma 2.6.

Corollary C.5. *For the parameters given in Lemma C.2, if* $T \geq \frac{\Delta_o L}{\kappa G^2}$*, then Robust-DGD* $\circ$ *ARC achieves*

$$\mathbb{E}\left[\left\|\nabla \mathcal{L}_{\mathcal{H}}\left(\hat{\theta}\right)\right\|^2\right] \leq 5\kappa \, \min\left\{G^2 + B^2\rho^2, \, \frac{G^2}{\max\{(1-\kappa B^2), 0\}}\right\},$$

where $\mathbb{E}\left[\cdot\right]$ *denotes the expectation over the choice of* $\hat{\theta}$*.*

Proof of Corollary C.5. For simplicity, we write $\mathcal{L}_{\mathcal{H}}$ as $\mathcal{L}$ throughout the proof.

Since $T \geq \frac{\Delta_o L}{\kappa G^2}$, $\gamma = \frac{\Delta_o}{\kappa G^2 T} \leq \frac{1}{L}$. Therefore, from Lemma C.2 we obtain that

$$\frac{1}{T}\sum_{t=1}^{T} \|\nabla \mathcal{L}(\theta_t)\|^2 \leq 5\kappa\left(G^2 + B^2\rho^2\right). \tag{29}$$

In the specific case when $\kappa B^2 < 1$, as $\gamma = \frac{\Delta_o}{\kappa G^2 T}$, from Lemma 2.6 we obtain that

$$\frac{1}{T}\sum_{t=1}^{T} \|\nabla \mathcal{L}(\theta_t)\|^2 \leq \frac{2\Delta_o}{(1-\kappa B^2)\gamma T} + \frac{\kappa G^2}{1-\kappa B^2} = \frac{3\kappa G^2}{1-\kappa B^2}. \tag{30}$$

Combining (29) and (30) we obtain that

$$\frac{1}{T}\sum_{t=1}^{T} \|\nabla \mathcal{L}(\theta_t)\|^2 \leq 5\kappa \min\left\{G^2 + B^2\rho^2, \, \frac{G^2}{1-\kappa B^2}\right\}.$$

Since $\mathbb{E}\left[\|\nabla \mathcal{L}(\theta_t)\|^2\right] = \frac{1}{T}\sum_{t=1}^{T} \|\nabla \mathcal{L}(\theta_t)\|^2$ (see Algorithm 1), the above concludes the proof. □

We are now ready to prove Theorem C.4. Recall that

$$\mathsf{BP} \coloneqq \frac{1}{2+B^2}, \quad \varepsilon_o \coloneqq \frac{1}{4} \cdot \frac{G^2(f/n)}{1-(2+B^2)(f/n)}, \quad \text{and}$$
$$\Psi(G, B, \rho) \coloneqq 640\left(1 + \frac{1}{B^2}\right)^2\left(1 + \frac{B^2\rho^2}{G^2}\right).$$

Proof of Theorem C.4. For simplicity, we write $\mathcal{L}_{\mathcal{H}}$ as $\mathcal{L}$ throughout the proof.

In the proof, we substitute $\mathsf{BP} = \frac{1}{2+B^2}$.

We first consider the case when $\frac{f}{n} = \frac{1-\xi}{2+B^2}$. In this particular case,

$$n = \left(\frac{2}{1-\xi} + \frac{B^2}{1-\xi}\right) f \geq \left(2 + \frac{B^2}{1-\xi}\right) f.$$

Therefore, thanks to Lemma 2.5, $\mathbf{F}$ is (f, κ)-robust with

$$\kappa \leq \frac{16f}{n-f}\left(1 + \frac{1-\xi}{B^2}\right)^2 = \frac{16(1-\xi)}{1+B^2+\xi}\left(1 + \frac{1-\xi}{B^2}\right)^2 \leq \frac{16(1-\xi)}{1+B^2}\left(1 + \frac{1}{B^2}\right)^2 \leq \kappa_o(1-\xi),$$

where $\kappa_o \coloneqq \frac{16}{1+B^2}\left(1 + \frac{1}{B^2}\right)^2$. Also, recall from the limitations of (f, κ)-robustness in Section 2 that

$$\kappa \geq \frac{f}{n-2f} \geq \frac{f}{n} \geq \frac{1-\xi_o}{2+B^2}.$$

Summarizing from above, we have

$$\frac{1-\xi_o}{2+B^2} \leq \kappa \leq \kappa_o(1-\xi). \tag{31}$$

This implies that

$$\rho \coloneqq \exp\left(\frac{(2+B^2)\Delta_o}{(1-\xi_o)G^2}L\right)\zeta \geq \exp\left(\frac{\Delta_o}{\kappa G^2}L\right)\zeta.$$

Therefore, since $\|\nabla\mathcal{L}_i(\theta_1)\| \leq \zeta$ for all $i \in \mathcal{H}$, the condition: $\max_{i\in\mathcal{H}}\|\nabla\mathcal{L}_i(\theta_1)\| \leq \exp\left(-\frac{\Delta_o}{\kappa G^2}L\right)\rho$ in Lemma C.2 is satisfied. Thus, by Corollary C.5 and (31) we obtain that

$$\mathbb{E}\left[\|\nabla\mathcal{L}(\theta_t)\|^2\right] \leq 5\kappa_o(1-\xi)(G^2+B^2\rho^2) = \frac{5\kappa_o(1-\xi)(G^2+B^2\rho^2)}{\frac{fG^2}{n-(2+B^2)f}}\frac{fG^2}{n-(2+B^2)f}. \tag{32}$$

Since $\frac{f}{n} = \frac{1-\xi}{2+B^2}$, we obtain that

$$\frac{5\kappa_o(1-\xi)(G^2+B^2\rho^2)}{\frac{fG^2}{n-(2+B^2)f}} = 5\kappa_o(1-\xi)(G^2+B^2\rho^2)\frac{\xi(2+B^2)}{G^2(1-\xi)} = 5\kappa_o\left(1+\frac{B^2\rho^2}{G^2}\right)\left(2+B^2\right)\xi.$$

Substituting κ_o from above, we obtain that

$$\begin{aligned}\frac{5\kappa_o(1-\xi)(G^2+B^2\rho^2)}{\frac{fG^2}{n-(2+B^2)f}} &= 80\left(\frac{2+B^2}{1+B^2}\right)\left(1+\frac{1}{B^2}\right)^2\left(1+\frac{B^2\rho^2}{G^2}\right)\xi \\ &\leq 160\left(1+\frac{1}{B^2}\right)^2\left(1+\frac{B^2\rho^2}{G^2}\right)\xi.\end{aligned}$$

Substituting from above in (32) concludes the proof for the first part of Theorem C.4.

The second part of Theorem C.4 follows immediately from the first inequality in (32), using the fact that $\kappa_o(1-\xi) \leq \kappa_o$. This concludes the proof. □

C.1 Assuming $\|\mathbf{F}(x_1,\ldots,x_n)\| \leq \max_{i\in[n]}\|x_i\|$ is Without Loss of Generality

Recall that we assume $\|\mathbf{F}(x_1,\ldots,x_n)\| \leq \max_{i\in[n]}\|x_i\|$ for all set of n vectors $x_1,\ldots,x_n \in \mathbb{R}^d$. In case this is not true, we can instead use the aggregation rule $\mathbf{F}^\dagger$ given by

$$\mathbf{F}^\dagger(x_1,\ldots,x_n) \coloneqq \mathrm{clip}_C\left(\mathbf{F}(x_1,\ldots,x_n)\right), \text{ where } C = \max_{i\in[n]}\|x_i\|.$$

This modification to the aggregation rule does not affect the learning guarantee. Specifically, due to the non-expansion property of $\mathrm{clip}_C(\cdot)$, for any non-empty set $S \subseteq [n]$, we have

$$\left\|\mathbf{F}^\dagger(x_1,\ldots,x_n) - \overline{x}_S\right\| \leq \left\|\mathbf{F}(x_1,\ldots,x_n) - \overline{x}_S\right\|,$$

where $\overline{x}_S \coloneqq \frac{1}{|S|}\sum_{i\in S} x_i$. Thus, if $\mathbf{F}$ is (f,κ)-robust, then $\mathbf{F}^\dagger$ is also (f,κ)-robust. Hence, we can make the above assumption on $\|\mathbf{F}(x_1,\ldots,x_n)\|$ without loss of generality.

D Comprehensive Experimental Setup

In this section, we present the comprehensive experimental setup considered in our paper.

D.1 Datasets and Heterogeneity

In our experiments, we consider three standard image classification datasets, namely MNIST Deng (2012), Fashion-MNIST Xiao et al. (2017), and CIFAR-10 Krizhevsky et al. (2014). To simulate data heterogeneity in our experiments, we make the honest workers sample from the datasets using a Dirichlet Hsu et al. (2019a) distribution of parameter α, as done in Hsu et al. (2019b); Allouah et al. (2023a); Farhadkhani et al. (2023). The smaller the α, the more heterogeneous

the setting. In our empirical evaluation, we set $\alpha \in \{0.1, 0.5, 1\}$ on (Fashion-)MNIST and $\alpha \in \{0.05, 0.075, 0.1, 0.2, 0.5\}$ on CIFAR-10 (refer to Figure 7). Furthermore, on MNIST and Fashion-MNIST, we also consider an *extreme* heterogeneity setting where the datapoints are sorted by increasing labels (0 to 9) and sequentially split equally among the honest workers.

The input images of MNIST are normalized with mean 0.1307 and standard deviation 0.3081, while the images of Fashion-MNIST are horizontally flipped. Moreover, CIFAR-10 is expanded with horizontally flipped images, followed by a per channel normalization with means 0.4914, 0.4822, 0.4465 and standard deviations 0.2023, 0.1994, 0.2010.

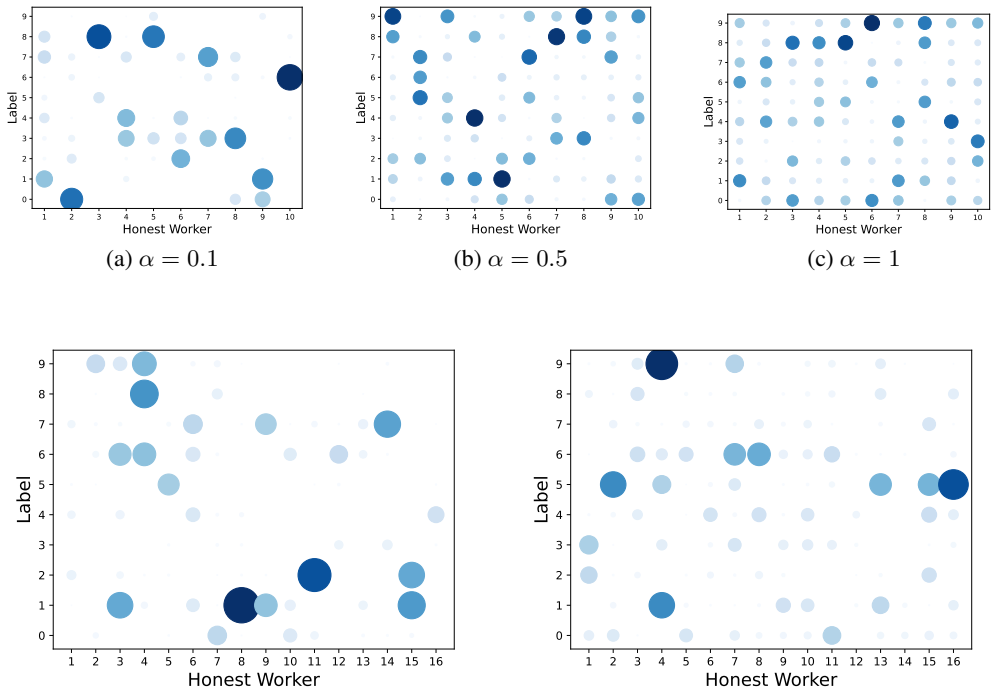

(a) $\alpha = 0.1$ (b) $\alpha = 0.5$ (c) $\alpha = 1$

(d) $\alpha = 0.075$ (e) $\alpha = 0.2$

Figure 7: Distribution of labels across honest workers on MNIST (row 1) and CIFAR-10 (row 2).

D.2 Algorithm, Distributed System, ML Models, and Hyperparameters

We perform our experiments using Robust-DSGD (see Algorithm 3), which is known to be an order-optimal robust variant of Robust-DGD Allouah et al. (2023a). On MNIST and Fashion-MNIST, we execute Robust-DSGD in a distributed system composed of $n - f = 10$ honest workers, and $f \in \{1, 2, 3, 4, 5, 7, 9\}$ adversarial workers. Furthermore, we train a convolutional neural network (CNN) of 431,080 parameters with batch size $b = 25$, $T = 1000$, $\gamma = 0.1$, and momentum parameter $\beta = 0.9$. Moreover, the negative log likelihood (NLL) loss function is used, along with an ℓ_2-regularization of 10^{-4}. On CIFAR-10, we execute Robust-DSGD using a CNN of 1,310,922 parameters, in a distributed system comprising $n - f = 16$ honest workers and $f = 1$ adversarial worker. We set $b = 50$, $T = 2000$, $\beta = 0.9$, and $\gamma = 0.05$ decaying once at step 1500. Finally, we use the NLL loss function with an ℓ_2 regularization of 10^{-2}.

In order to present the architectures of the ML models used in our experiments, we adopt the following compact terminology introduced in Allouah et al. (2023a).

L(#outputs) represents a **fully-connected linear layer**, R stands for **ReLU activation**, S stands for **log-softmax**, C(#channels) represents a *fully-connected 2D-convolutional layer* (kernel size 5, padding 0, stride 1), M stands for **2D-maxpool** (kernel size 2), B stands for **batch-normalization**, and D represents **dropout** (with fixed probability 0.25).

Algorithm 3 Robust Distributed Stochastic Gradient Descent (Robust-DSGD)

Input: **Server** chooses an initial model $\theta_1 \in \mathbb{R}^d$, *learning rate* $\gamma \in \mathbb{R}^+$, robust aggregation $\mathbf{F} : \mathbb{R}^{n \times d} \to \mathbb{R}^d$, *momentum parameter* $\beta \in \mathbb{R}^+$. Each **honest worker** w_i sets an initial *momentum* $m_0^{(i)} = 0 \in \mathbb{R}^d$.
for $t = 1$ to T **do**
  Server broadcasts θ_t to all workers.
  for each honest worker w_i **in parallel do**
    Sample a random data point $z^{(i)}$ uniformly from $\mathcal{D}_i$.
    Compute stochastic gradient $g_t^{(i)} := \nabla \ell(\theta_t, z^{(i)})$.
    Update momentum: $m_t^{(i)} := (1-\beta) g_t^{(i)} + \beta m_{t-1}^{(i)}$.
    Send $m_t^{(i)}$ to **Server**.
    // An adversarial worker w_j can send an arbitrary vector in $\mathbb{R}^d$ for $m_t^{(j)}$
  end for
  Server computes $R_t := \mathbf{F}\left(m_t^{(1)}, \ldots, m_t^{(n)}\right)$.
  Server updates the model: $\theta_{t+1} := \theta_t - \gamma R_t$.
end for
Output: **Server** outputs $\hat{\theta}$ chosen uniformly at random from $\{\theta_1, \ldots, \theta_T\}$.

The comprehensive experimental setup, as well as the architecture of the models, are presented in Table 2.

Dataset	(Fashion-)MNIST	CIFAR-10
Data heterogeneity	$\alpha \in \{0.1, 0.5, 1\}$ and extreme	$\alpha \in \{0.05, 0.075, 0.1, 0.2, 0.5\}$
Model type	CNN	CNN
Model architecture	C(20)-R-M-C(20)-R-M-L(500)-R-L(10)-S	(3,32×32)-C(64)-R-B-C(64)-R-B-M-D-C(128)-R-B-C(128)-R-B-M-D-L(128)-R-D-L(10)-S
Number of parameters	431,080	1,310,922
Loss	NLL	NLL
ℓ_2-regularization	10^{-4}	10^{-2}
Number of steps	$T = 1000$	$T = 2000$
Learning rate	$\gamma = 0.1$	$\gamma_t = \begin{cases} 0.05 & t \leq 1500 \\ 0.00082 & 1500 < t \leq 2000 \end{cases}$
Momentum parameter	$\beta = 0.9$	$\beta = 0.9$
Batch size	$b = 25$	$b = 50$
Honest workers	$n - f = 10$	$n - f = 16$
Adversarial workers	$f \in \{1, 2, 3, 4, 5, 7, 9\}$	$f = 1$

Table 2: Experimental setup on (Fashion-)MNIST and CIFAR-10

D.3 BYZANTINE ATTACKS

In our experiments, the adversarial workers execute five state-of-the-art adversarial attacks from the Byzantine ML literature, namely *sign-flipping* (SF) Allen-Zhu et al. (2020), *label-flipping* (LF) Allen-Zhu et al. (2020), *mimic* Karimireddy et al. (2022), *fall of empires* (FOE) Xie et al. (2020), and *a little is enough* (ALIE) Baruch et al. (2019).

The exact functionality of the attacks is detailed below. In every step t, let $\overline{m}_t$ be an estimation of the true honest momentum at step t. In our experiments, we estimate $\overline{m}_t$ by averaging the momentums sent by the honest workers in step t of Robust-DSHB. In other words, $\overline{m}_t = \frac{1}{|\mathcal{H}|} \sum_{i \in \mathcal{H}} m_t^{(i)}$, where $m_t^{(i)}$ is the momentum computed by honest worker w_i in step t.

- SF: the adversarial workers send the vector $-\overline{m}_t$ to the server.
- LF: the adversarial workers compute their gradients on flipped labels, and send the flipped gradients to the server. Since the original labels l for (Fashion-)MNIST and CIFAR-10 are in $\{0, ..., 9\}$, the adversarial workers execute a label flip/rotation by computing their gradients on the modified labels $l' = 9 - l$.
- Mimic: the adversarial workers *mimic* a certain honest worker by sending its gradient to the server. In order to determine the optimal honest worker for the adversarial workers to mimic, we use the heuristic in Karimireddy et al. (2022).
- FOE: the adversarial workers send $(1 - \tau)\overline{m}_t$ in step t to the server, where $\tau \geq 0$ is a fixed real number representing the attack factor. When $\tau = 2$, this attack is equivalent to SF.
- ALIE: the adversarial workers send $\overline{m}_t + \tau\sigma_t$ in step t to the server, where $\tau \geq 0$ is a fixed real number representing the attack factor, and σ_t is the coordinate-wise standard deviation of $\overline{m}_t$.

Since the FOE and ALIE attacks have τ as parameter, we implement in our experiments enhanced and adaptive versions of these attacks, where the attack factor is not constant and may be different in every iteration. In every step t, we determine the optimal attack factor τ_t through a grid search over a predefined range of values. More specifically, in every step t, τ_t takes the value that maximizes the damage inflicted by the adversarial workers, i.e., that maximizes the l^2 norm of the difference between the average of the honest momentums $\overline{m}_t$ and the output of the aggregation R_t at the server.

D.4 BENCHMARKING AND REPRODUCIBILITY

We evaluate the performance of ARC compared to no clipping within the context of Robust-DSGD. Accordingly, we choose $\mathbf{F} \circ$ NNM as aggregator in Algorithm 1, where $\mathbf{F} \in \{$CWTM, GM, CWMed, MK$\}$ is an aggregation rule proved to be (f, κ)-robust Allouah et al. (2023a). Composing these aggregation rules with NNM provides them with optimal (f, κ)-robustness Allouah et al. (2023a). As benchmark, we also execute the standard DSGD algorithm in the same setting, but in the absence of adversarial workers (i.e., without attack and $f = 0$). We plot in Table 1 and Figures 2a and 4 the metric of ***worst-case maximal accuracy***. In other words, for each of the aforementioned five Byzantine attacks, we record the maximal accuracy achieved by Robust-DSGD during the learning under that attack. The *worst-case maximal accuracy* is thus the *smallest* maximal accuracy encountered across the five attacks. As the attack executed by adversarial workers cannot be known in advance in a practical system, this metric is critical to accurately evaluate the robustness of aggregation methods, as it gives us an estimate of the potential worst-case performance of the algorithm. Finally, all our experiments are run with seeds 1 to 5 for reproducibility purposes. We provide standard deviation measurements for all our results (across the five seeds). In Appendix E, we show the performance of our algorithm (compared to no clipping) in worst-case maximal accuracy, when varying the heterogeneity level or the number of adversarial workers f. We also show some plots showing the evolution of the learning with time under specific attacks (e.g., Figures 10, 11, 12, and 16 in Appendix E), but the totality of these plots can be found in the supplementary material (attached in a folder per dataset).

E ADDITIONAL EXPERIMENTAL RESULTS

In this section, we complete the experimental results that could not be placed in the main paper.

E.1 MNIST

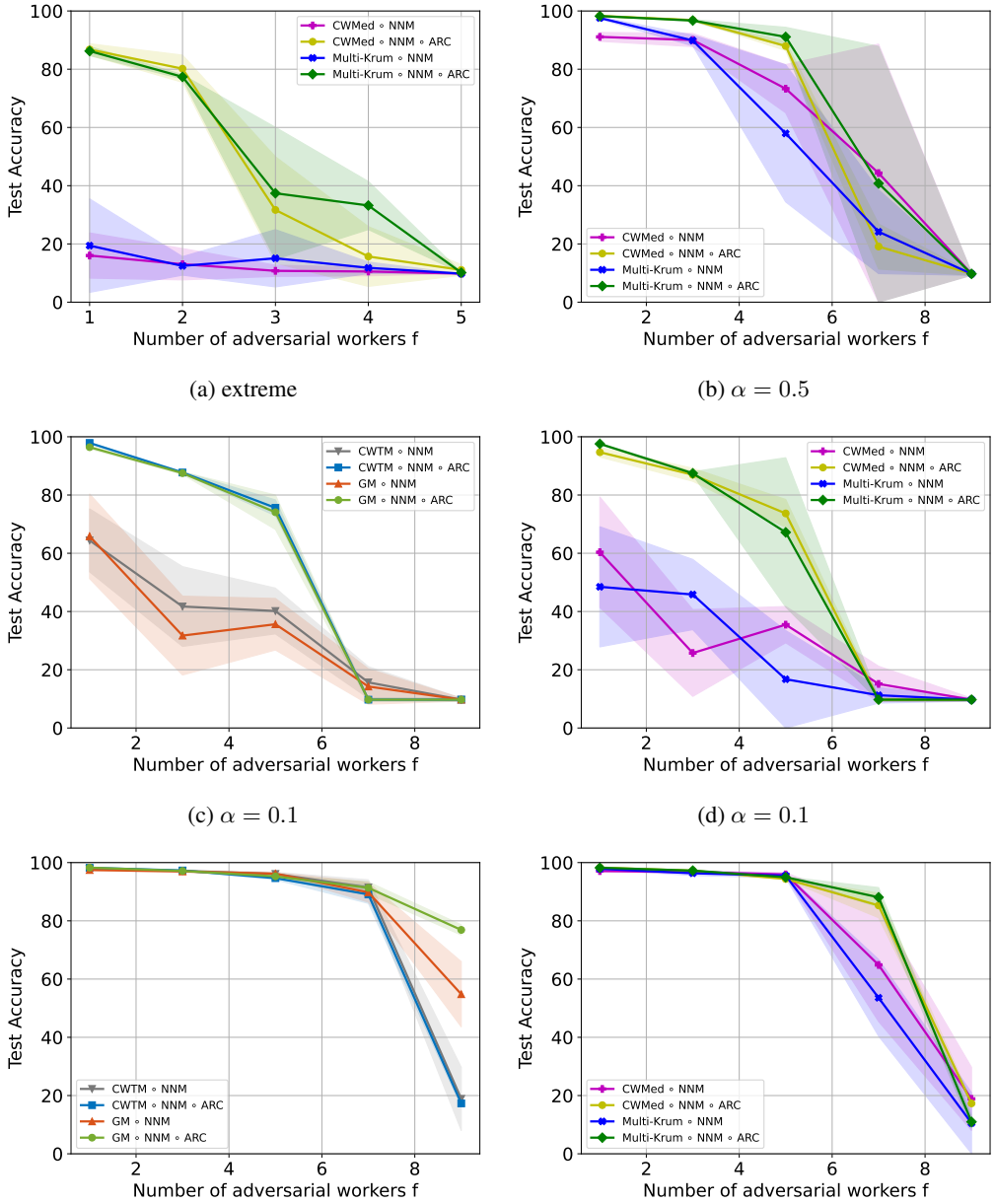

(a) extreme

(b) $\alpha = 0.5$

(c) $\alpha = 0.1$

(d) $\alpha = 0.1$

(e) $\alpha = 1$

(f) $\alpha = 1$

Figure 8: *Worst-case maximal accuracies* achieved by Robust-DSGD when using ARC compared to no clipping, on heterogeneously-distributed MNIST with 10 honest workers. We fix the heterogeneity level, and vary the the number of Byzantine workers f.

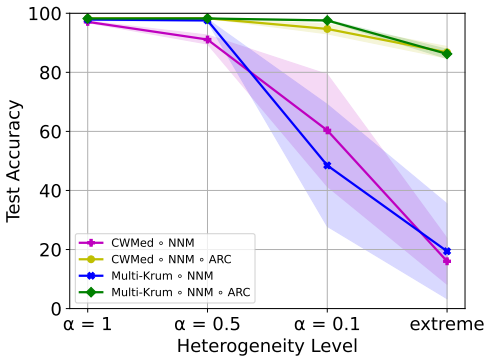

(a) $f = 1$

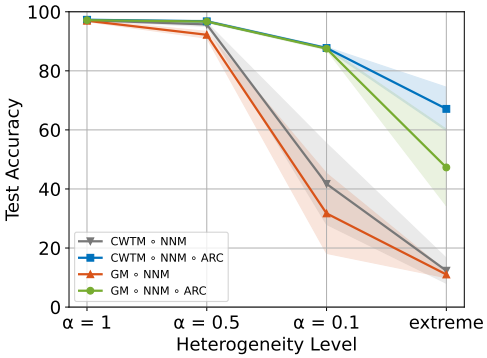

(b) $f = 3$

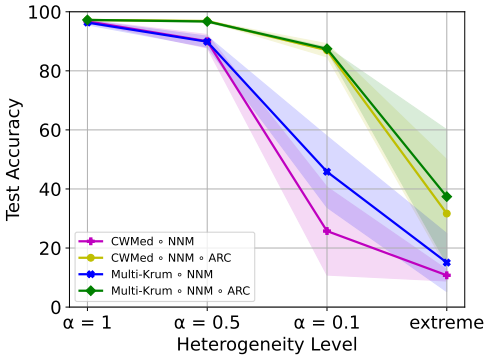

(c) $f = 3$

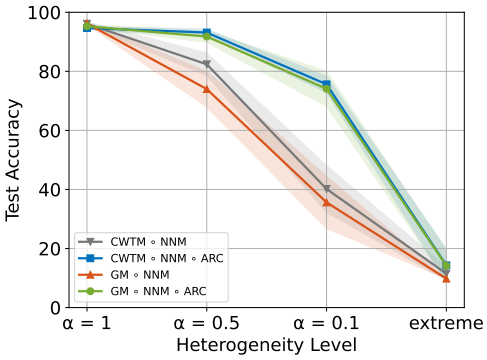

(d) $f = 5$

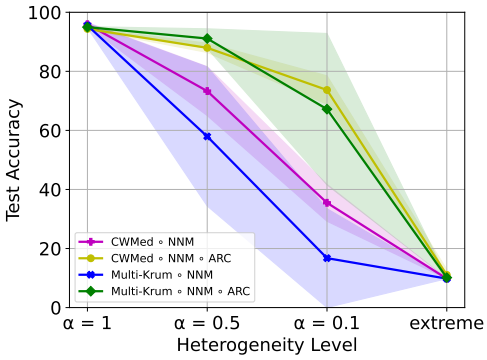

(e) $f = 5$

Figure 9: *Worst-case maximal accuracies* achieved by Robust-DSGD when using ARC compared to no clipping, on heterogeneously-distributed MNIST with 10 honest workers. We fix the number of Byzantine workers f, and vary the heterogeneity level.

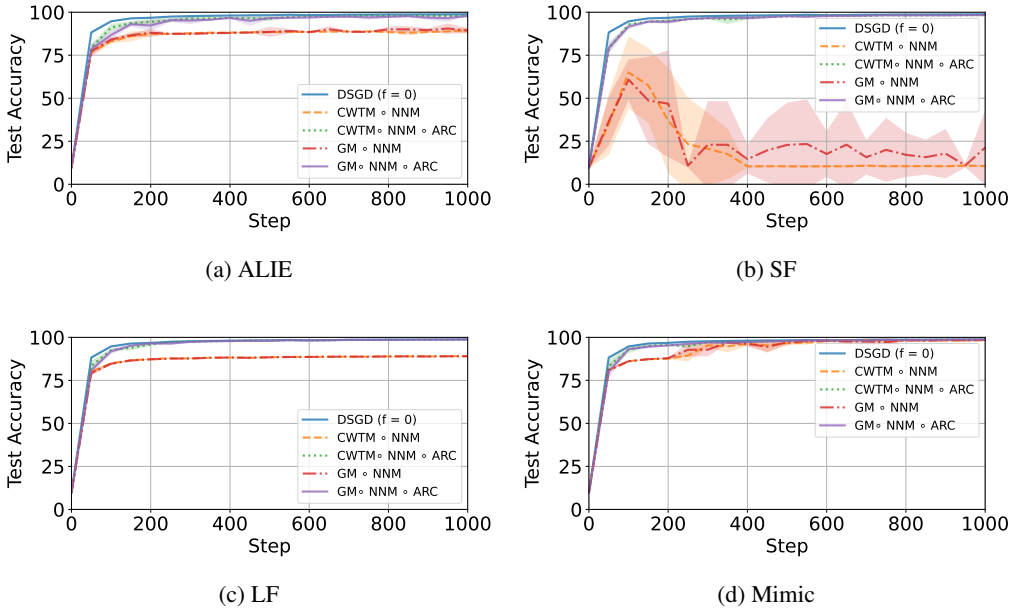

(a) ALIE (b) SF

(c) LF (d) Mimic

Figure 10: Performance of Robust-DSGD when using ARC compared to no clipping, on heterogeneously-distributed MNIST (extreme heterogeneity) with 10 honest workers and $f = 1$, under several attacks. This complements Figure 3c of the main paper.

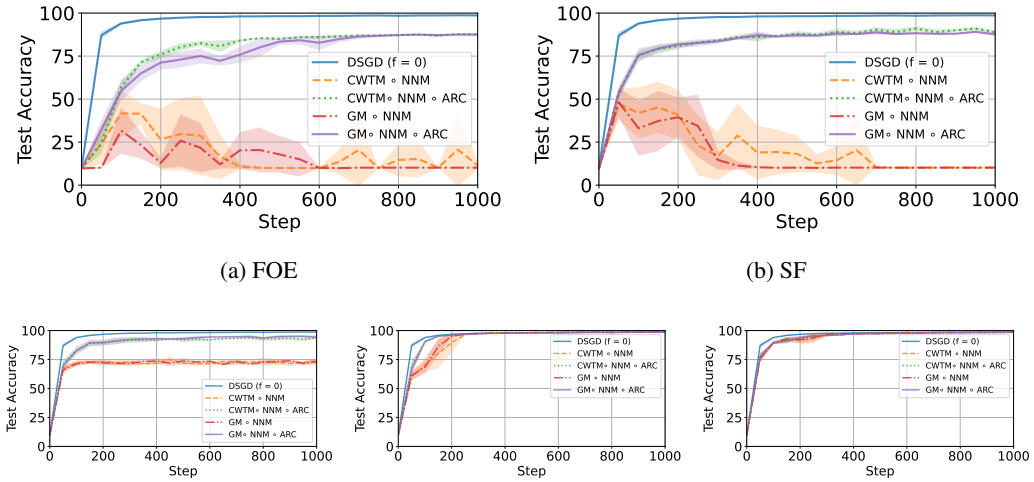

(a) FOE (b) SF

(c) ALIE (d) LF (e) Mimic

Figure 11: Performance of Robust-DSGD when using ARC compared to no clipping, on heterogeneously-distributed MNIST ($\alpha = 0.1$) with 10 honest workers and $f = 3$, under several attacks.

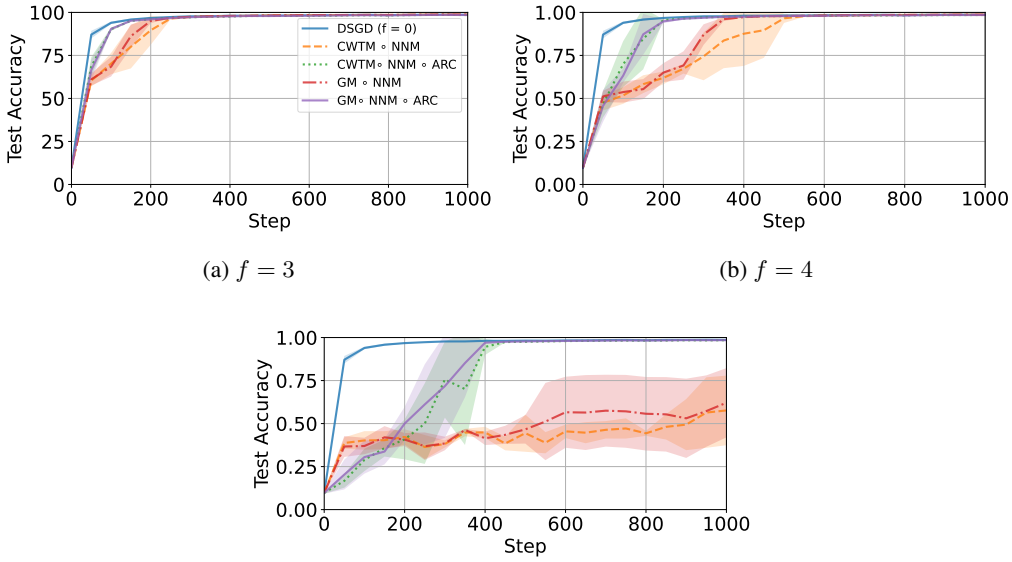

(a) $f = 3$

(b) $f = 4$

(c) $f = 5$

Figure 12: Performance of Robust-DSGD under the LF attack when using ARC compared to no clipping, on heterogeneously-distributed MNIST ($\alpha = 0.1$) with 10 honest workers and varying number of adversarial workers f.

E.2 FASHION-MNIST

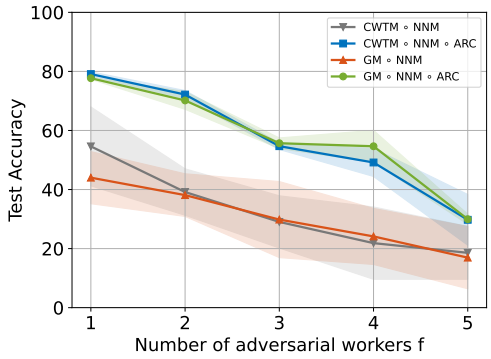

(a) $\alpha = 0.1$

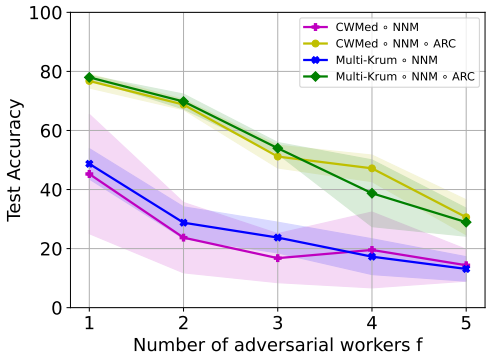

(b) $\alpha = 0.1$

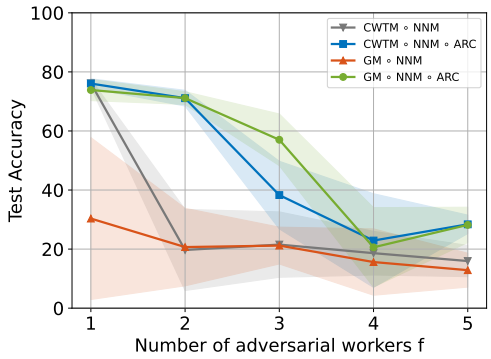

(c) $\alpha = 0.05$

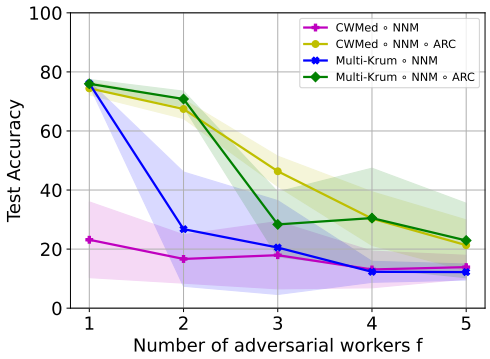

(d) $\alpha = 0.05$

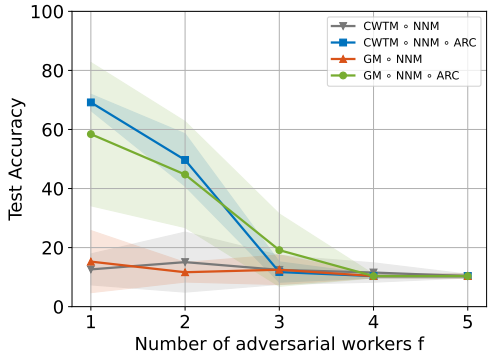

(e) extreme

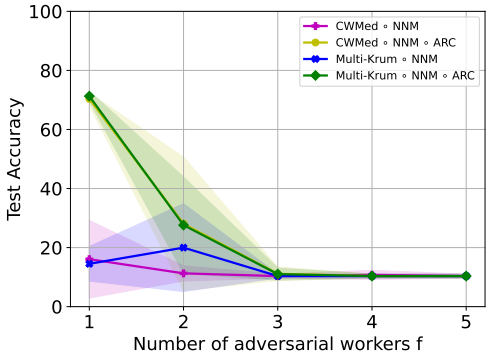

(f) extreme

Figure 13: *Worst-case maximal accuracies* achieved by Robust-DSGD when using ARC compared to no clipping, on heterogeneously-distributed Fashion-MNIST with 10 honest workers. We fix the heterogeneity level and vary the number of adversarial workers f.

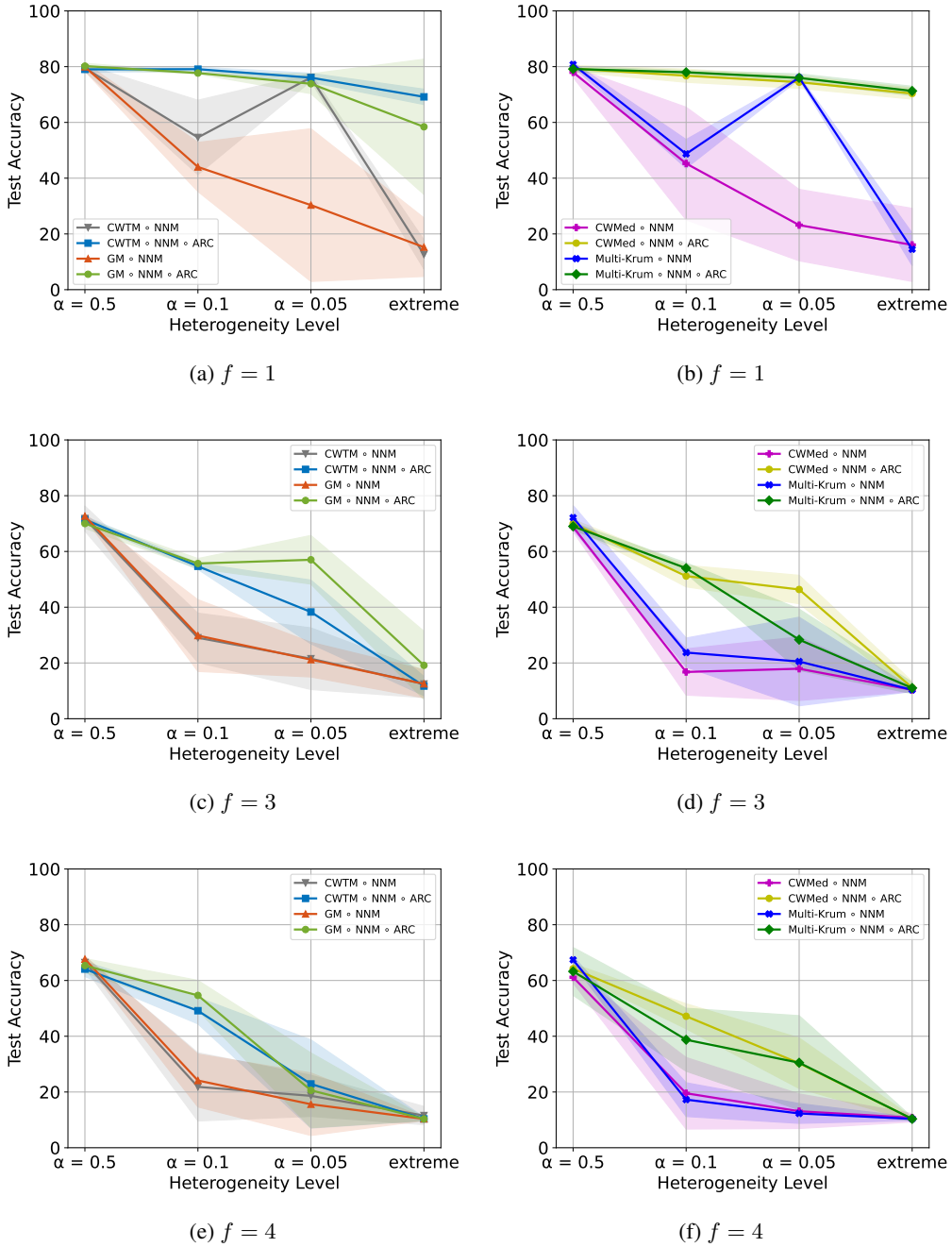

(a) $f = 1$ (b) $f = 1$

(c) $f = 3$ (d) $f = 3$

(e) $f = 4$ (f) $f = 4$

Figure 14: *Worst-case maximal accuracies* achieved by Robust-DSGD when using ARC compared to no clipping, on heterogeneously-distributed Fashion-MNIST with 10 honest workers. We fix the number of adversarial workers f and vary the heterogeneity level.

E.3 CIFAR-10

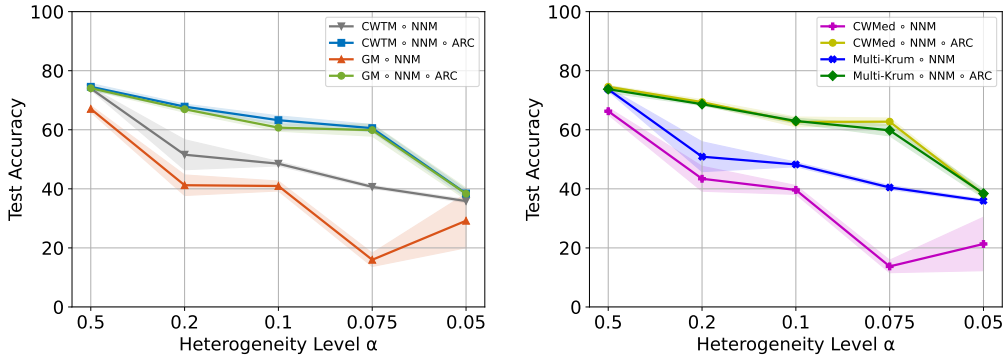

(a) $f = 1$ (b) $f = 1$

Figure 15: *Worst-case maximal accuracies* achieved by Robust-DSGD when using ARC compared to no clipping, on heterogeneously-distributed CIFAR-10 with 16 honest workers. We fix the number of adversarial workers $f = 1$ and vary the heterogeneity level.

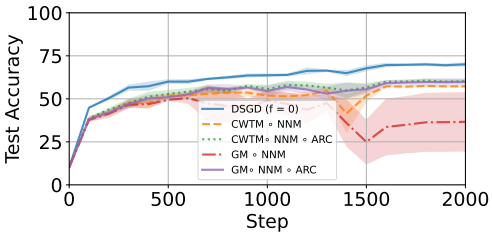

(a) ALIE with CWTM and GM

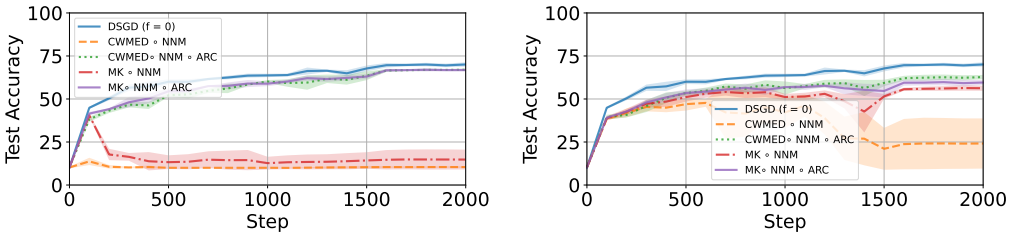

(b) FOE with CWMED and MK (c) ALIE with CWMED and CWMED

Figure 16: *Worst-case maximal accuracies* achieved by Robust-DSGD when using ARC compared to no clipping, on heterogeneously-distributed CIFAR-10 ($\alpha = 0.075$) with 16 honest workers and $f = 1$ executing ALIE and FOE. This figure complements Figure 5 in the main paper.

F Static Clipping vs ARC

In this section, we present empirical results on static clipping when used as a pre-aggregation technique in Robust-DSGD, and compare its performance to our proposed adaptive algorithm ARC.

F.1 Limitations of Static Clipping

We perform our experiments using Robust-DSGD (see Algorithm 3) on (Fashion-)MNIST and CIFAR-10. We consider three different levels of heterogeneity, that we call *moderate* (corresponding

to sampling from a Dirichlet distribution of parameter $\alpha = 1$), *high* ($\alpha = 0, 1$), and *extreme* (as explained in Appendix D). On MNIST and Fashion-MNIST, we execute Robust-DSGD in a distributed system composed of $n = 15$ workers, among which $f \in \{3, 4\}$ are Byzantine. Furthermore, we train a convolutional neural network of 431,080 parameters with batch size $b = 25$, $T = 1000$, $\gamma = 0.1$, and momentum parameter $\beta = 0.9$. Moreover, the negative log likelihood loss function is used, along with an ℓ_2-regularization of 10^{-4}. On CIFAR-10, we execute Robust-DSGD on ResNet-18 He et al. (2015), in a distributed system comprising $n = 9$ workers among which $f \in \{1, 2\}$ are Byzantine. We set $b = 128$, $T = 2000$, $\beta = 0.9$, and $\gamma = 0.1$ decaying once by $10\times$ at step 1500. Finally, we use the cross-entropy loss function with an ℓ_2 regularization of 5×10^{-4}.

In our experiments, we examine a wide range of static clipping parameters. Specifically, we choose $C \in \{0.02, 0.2, 2, 20\}$ on MNIST.

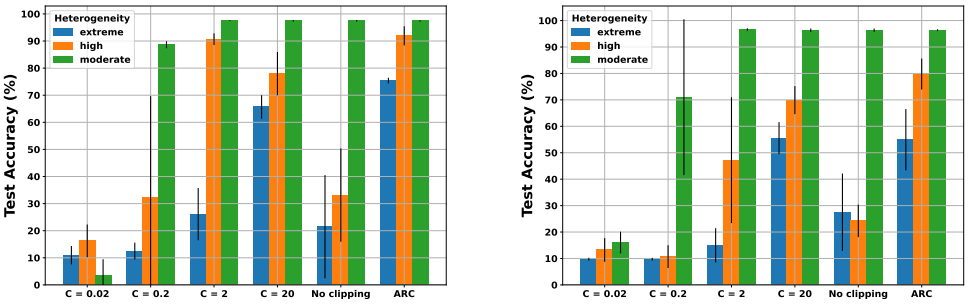

(a) $f = 3$ (b) $f = 4$

Figure 17: Impact of the clipping strategy and heterogeneity level on the ***worst-case maximal accuracy*** achieved by Robust-DSGD against five Byzantine attacks on heterogeneous MNIST with $n = 15$ workers. CWTM $\circ$ NNM is used as aggregation. DSGD reaches at least 98.5% in accuracy in all heterogeneity regimes.

Unreliability due to the attack. First, the efficacy of static clipping is significantly influenced by the type of Byzantine attack executed during the learning process. To illustrate, while $C = 2$ exhibits the best performance under the SF attack Allen-Zhu et al. (2020), depicted in Figure 1, it leads to a complete collapse of learning under LF Allen-Zhu et al. (2020). Consequently, identifying a static clipping threshold C that consistently performs well in practice against any attack is difficult (if not impossible). This highlights the fragility of static clipping, as the unpredictable nature of the Byzantine attack, a parameter that cannot be a priori known, can significantly degrade the performance of the chosen static clipping approach.

Unreliability due to the heterogeneity model. Second, the robustness under static clipping is notably influenced by the level of heterogeneity present across the datasets of honest workers. To illustrate this impact, we present in Figure 17 the performances of Robust-DSGD for different levels of heterogeneity (moderate, high, and extreme) and different values of C. In the left plot of Figure 17, $C = 2$ emerges as the best static clipping threshold when the heterogeneity is high whereas $C = 20$ appears to be sub-optimal. On the other hand, under extreme heterogeneity, the accuracy associated to $C = 2$ diminishes drastically while $C = 20$ becomes a better choice. Intuitively, in heterogeneous scenarios, honest gradients become large in l^2-norm, due to the increasingly detrimental effect of Byzantine attacks. Consequently, we must increase the static clipping threshold. Failing to do so could introduce a significant bias. More details on this observation can be found in Figure 18. This highlights the intricate dependence of the performance of static clipping on data heterogeneity, and emphasizes the necessity to fine-tune static clipping strategies prior to the learning.

Unreliability due to the number of Byzantine workers. Last but not least, the number of Byzantine workers f also affects the efficacy of static clipping. As seen in Figure 17, $C = 2$ leads to the highest accuracy among static clipping strategies when $f = 3$ in high heterogeneity, but cannot be used when $f = 4$ as its corresponding accuracy drops below 50% (see right plot of Figure 17).

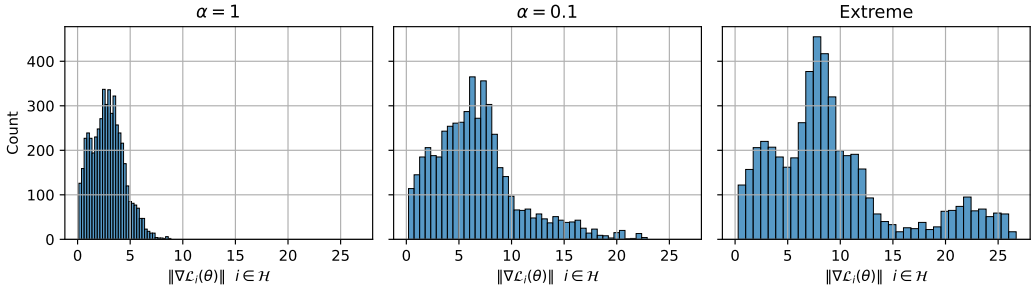

Figure 18: Distribution of the norms of honest gradients during the learning on heterogeneous MNIST. There are $f = 3$ Byzantine workers (among $n = 15$) executing the LF attack. CWTM $\circ$ NNM is used as aggregation method.

Overall, our empirical findings reveal that there is no single value of C for which static clipping consistently delivers satisfactory performance across the various settings. We have also shown that the performance of static clipping is greatly influenced on typically uncontrollable parameters, such as data heterogeneity and the nature of the Byzantine attack. Indeed, it should be noted that explicitly estimating these parameters is challenging (if not impossible) in a distributed setting. First, since the server does not have direct access to the data, it cannot estimate the degree of heterogeneity. Second, as (by definition) a Byzantine worker can behave in an unpredictable manner, we cannot adjust C to the attack(s) being executed by the Byzantine workers. This highlights the necessity for a robust clipping alternative that can naturally adapt to the setting in which it is deployed.

F.2 Empirical Benefits of ARC

In contrast to static clipping, ARC is adaptive, delivering consistent performance across diverse levels of heterogeneity, Byzantine attacks, and number of Byzantine workers.

Adaptiveness. ARC dynamically adjusts its clipping parameter C_t based on the norms of honest momentums at step t, avoiding static over-clipping or under-clipping. This adaptability is evident in Figure 19, where C_t consistently decreases with time under all attacks, an expected behavior when reaching convergence. Moreover, Figure 19 also illustrates that any surge in the norm of the honest mean corresponds to a direct increase in C_t, highlighting the adaptive nature of ARC.

Robust performance across heterogeneity regimes. The efficacy of our solution is illustrated in Figure 17, showcasing a consistently robust performance for all considered heterogeneity levels. Specifically, in scenarios of moderate heterogeneity where clipping may not be essential, ARC matches the performance of *No clipping* as well as static strategies $C = 2$ and $C = 20$. Conversely, the left plot of Figure 17 shows that under high and extreme heterogeneity, ARC surpasses the best static clipping strategy in terms of accuracy, highlighting the effectiveness of our approach.

Robust performance across Byzantine regimes. ARC exhibits robust performance across diverse Byzantine scenarios, encompassing variations in both the type of Byzantine attack and the number of Byzantine workers f. As depicted in Figures 1 and 17, ARC consistently yields robust performance, regardless of the Byzantine attack. In extreme heterogeneity with $f = 3$, ARC maintains an accuracy of 75%, while $C = 2$ demonstrates a subpar worst-case accuracy of 25% (also refer to the right plot of Figure 1). Furthermore, despite the increase in the number of Byzantine workers to $f = 4$, ARC remains the top-performing clipping approach among all considered strategies.

This analysis underscores the empirical superiority of ARC over static clipping methods, eliminating the reliance on data heterogeneity and the specific Byzantine regime. Similar trends are also observed in Figure 20, when executing Robust-DSGD using other aggregation methods such as CWMed $\circ$ NNM, GM $\circ$ NNM, and Multi-Krum $\circ$ NNM.

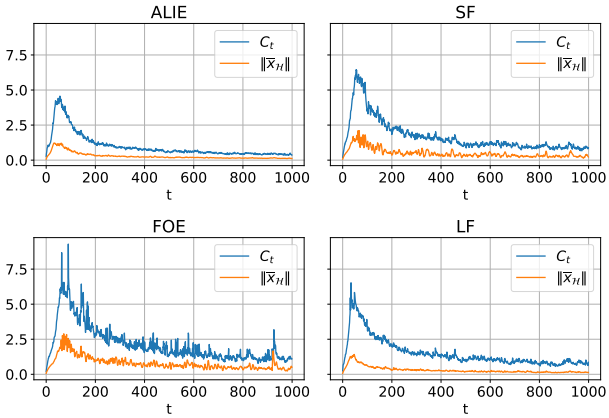

Figure 19: Evolution of the adaptive clipping parameter C_t of ARC compared to the norm of the honest mean during the learning on heterogeneous MNIST ($\alpha = 1$). There are $f = 3$ Byzantine workers among $n = 15$. CWTM $\circ$ NNM is used as aggregation. ARC dynamically adjusts its clipping parameter C_t based on the norms of honest momentums at step t, avoiding static over-clipping or under-clipping. This adaptability is evident in under all attacks, where C_t consistently decreases with time, an expected behavior when reaching convergence.

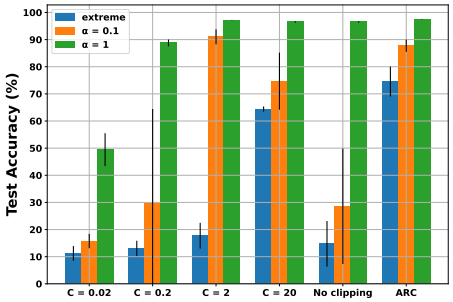

(a) CWMed $\circ$ NNM

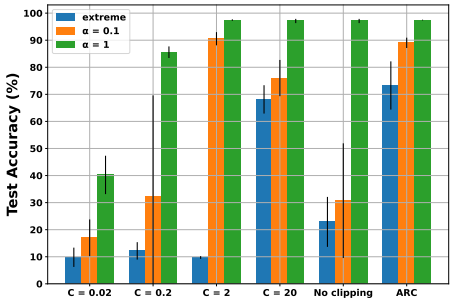

(b) GM $\circ$ NNM

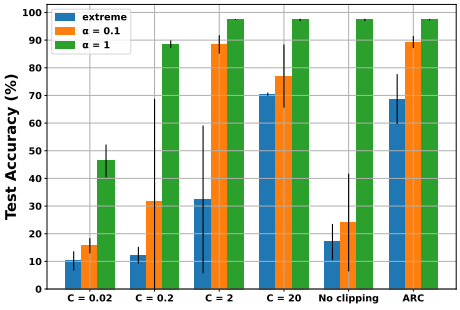

(c) MK $\circ$ NNM

Figure 20: Impact of the clipping strategy on the worst-case maximal accuracy achieved during the learning against five Byzantine attacks on heterogeneous MNIST, with $f = 3$ and $n = 15$.

G ADDITIONAL EXPERIMENTS (REBUTTAL)

G.1 EXPERIMENTS ON LARGE SYSTEMS - 30 HONEST WORKERS

We consider training on the MNIST dataset in a larger system comprised of $n - f = 30$ honest workers, and $f \in \{3, 6, 9\}$ Byzantine workers.

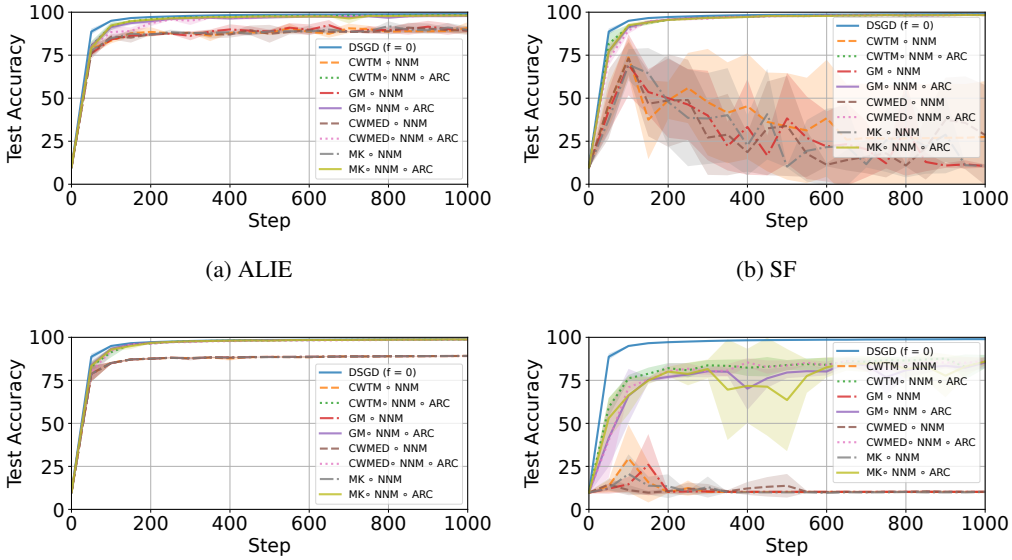

(a) ALIE (b) SF

(c) LF (d) FOE

Figure 21: Performance of Robust-DSGD when using ARC and without clipping on distributed MNIST under *extreme* heterogeneity. There are $f = 3$ adversarial workers executing 4 attacks.

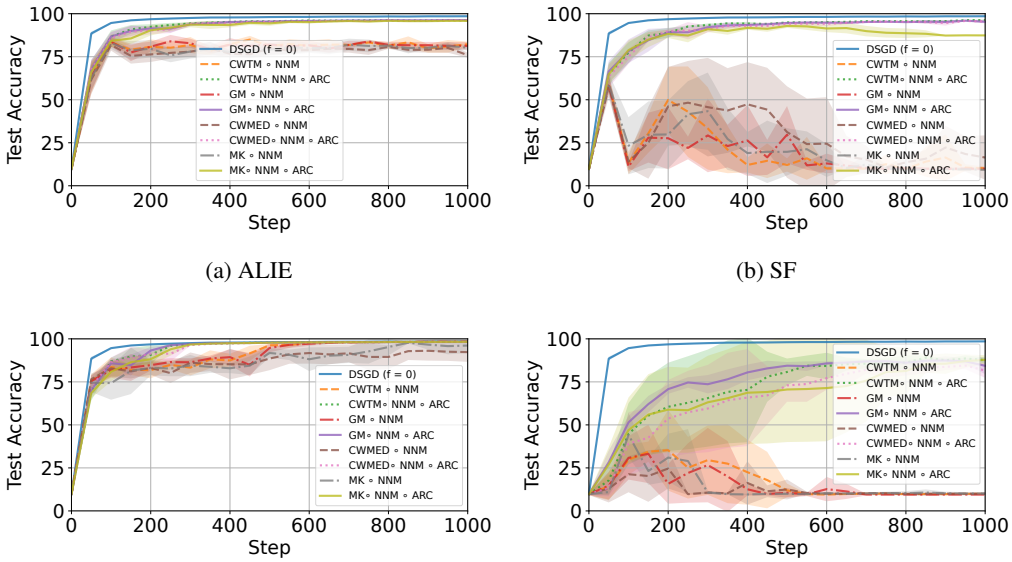

(a) ALIE (b) SF

(c) LF (d) FOE

Figure 22: Performance of Robust-DSGD when using ARC and without clipping on heterogeneously-distributed MNIST with $\alpha = 0.1$. There are $f = 9$ adversarial workers executing 4 attacks.

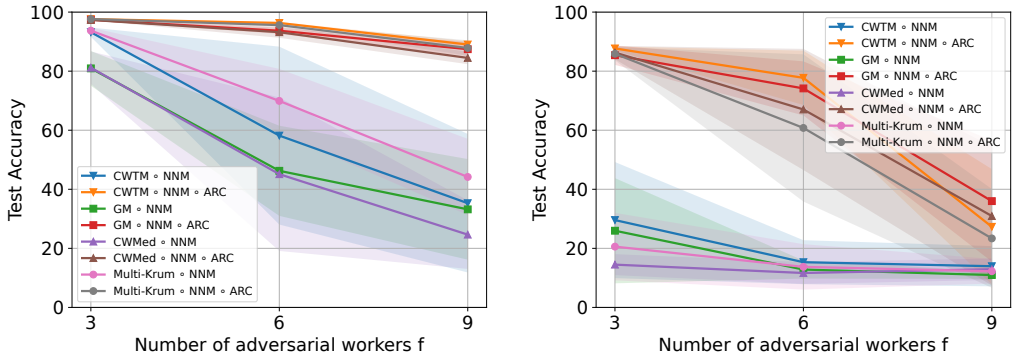

(a) $\alpha = 0.1$ (b) extreme heterogeneity

Figure 23: *Worst-case maximal accuracies* achieved by Robust-DSGD, with and without ARC, on heterogeneously-distributed MNIST with 30 honest workers. We consider a heterogeneous data distribution with $\alpha = 0.1$ (*left*) and extreme heterogeneity (*right*), and vary $f \in \{3, 6, 9\}$.

G.2 Runtime Comparison - NNM vs ARC

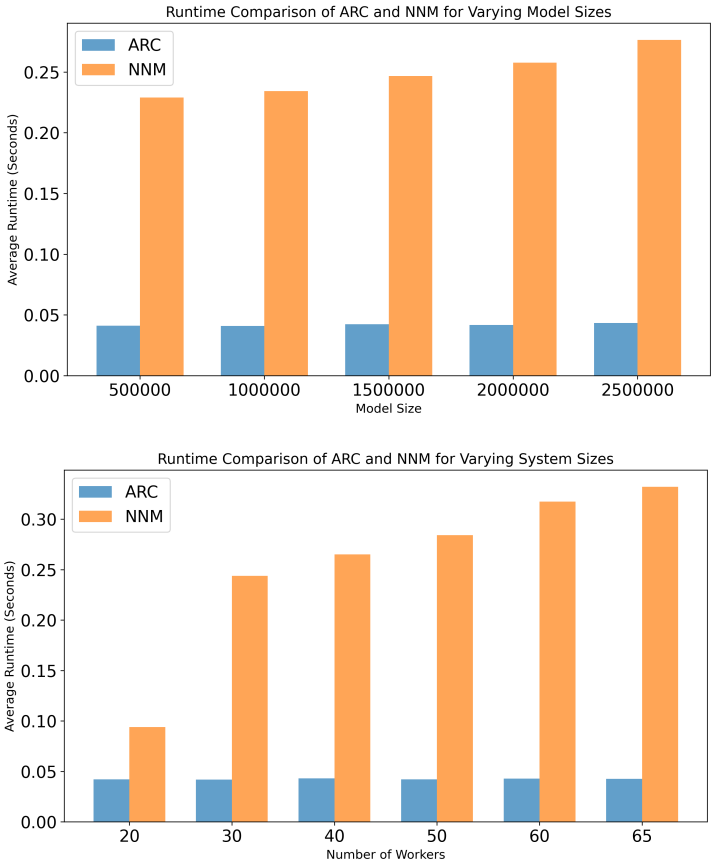

Figure 24: Computational performance of ARC vs NNM, in two different settings. In the first plot, we fix the number of workers $n = 30$, $f = 3$, and vary the model size d. In the second plot, we fix the model size $d = 1310922$ (the size of the model we used on CIFAR-10) and $f = 3$, and vary the number of workers in the distributed system.

G.3 Additional Experiments on CIFAR-10

G.3.1 Initial System With Larger f

We run experiments on CIFAR-10, with $n - f = 16$ honest workers, and $f \in \{2, 3\}$ Byzantine workers. We consider heterogeneity regimes of $\alpha = 0.2$ and 0.5, when $f = 2$ and 3, respectively. The results are presented in Table 3, and we show in Figures 25 and 26 the performance of ARC compared to no clipping under the FOE attack.

	$f = 2, \alpha = 0.2$		$f = 3, \alpha = 0.5$	
Aggregation	No Clipping	ARC	No Clipping	ARC
CWTM $\circ$ NNM	44.3 ± 5.2	$\mathbf{53.0 \pm 4.7}$	52.0 ± 1.3	$\mathbf{55.4 \pm 1.1}$
GM $\circ$ NNM	33.8 ± 6.7	$\mathbf{50.2 \pm 3.3}$	50.9 ± 2.5	$\mathbf{49.6 \pm 1.4}$
CWMed $\circ$ NNM	32.6 ± 9.8	$\mathbf{49.7 \pm 2.7}$	48.7 ± 2.4	$\mathbf{62.7 \pm 0.9}$
MK $\circ$ NNM	45.0 ± 4.2	$\mathbf{51.9 \pm 2.1}$	50.3 ± 1.4	$\mathbf{50.2 \pm 2.4}$

Table 3: *Worst-case maximal accuracies* (%) achieved by Robust-DSGD on heterogeneously-distributed CIFAR-10 with ARC and without. There are $f \in \{2, 3\}$ adversarial workers with $n - f = 16$ honest workers.

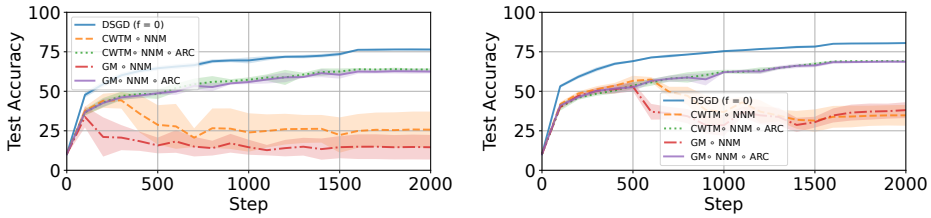

(a) $f = 2, \alpha = 0.2$ (b) $f = 3, \alpha = 0.5$

Figure 25: Performance of Robust-DSGD when using ARC and without clipping on CIFAR-10. There are 16 honest workers, and $f = 2$ (left) and $f = 3$ (right) adversarial workers executing the **FOE** attack. The aggregations used are CWTM $\circ$ NNM and GM $\circ$ NNM.

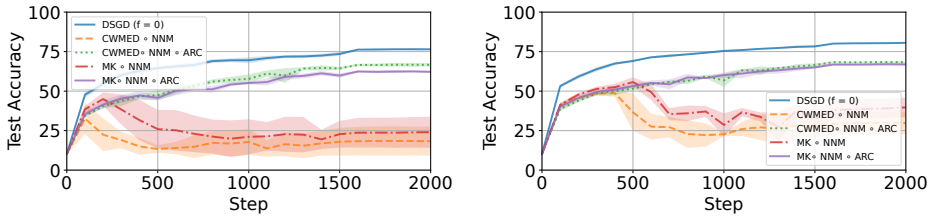

(a) $f = 2, \alpha = 0.2$ (b) $f = 3, \alpha = 0.5$

Figure 26: Performance of Robust-DSGD when using ARC and without clipping on CIFAR-10. There are 16 honest workers, and $f = 2$ (left) and $f = 3$ (right) adversarial workers executing the **FOE** attack. The aggregations used are CWMED $\circ$ NNM and MK $\circ$ NNM.

G.3.2 Larger System - 33 Honest Workers

We also run experiments on CIFAR-10 in a larger system comprised of $n - f = 33$ honest workers, and $f = 2$ and 3 Byzantine workers. We consider the high heterogeneity regime of $\alpha = 0.1$. The results are presented in Table 4, and we show in Figures 27 and 28 the performance of ARC compared to no clipping under the FOE attack.

	$f = 2$		$f = 3$	
Aggregation	No Clipping	ARC	No Clipping	ARC
CWTM $\circ$ NNM	45.5 ± 1.3	$\mathbf{54.2} \pm \mathbf{1.0}$	41.3 ± 0.5	$\mathbf{47.5} \pm \mathbf{1.5}$
GM $\circ$ NNM	41.8 ± 1.1	$\mathbf{55.2} \pm \mathbf{2.2}$	40.0 ± 1.2	$\mathbf{47.5} \pm \mathbf{1.5}$
CWMed $\circ$ NNM	42.5 ± 1.42	$\mathbf{54.7} \pm \mathbf{1.2}$	35.7 ± 8.7	$\mathbf{49.7} \pm \mathbf{3.4}$
MK $\circ$ NNM	45.8 ± 0.8	$\mathbf{54.8} \pm \mathbf{2.5}$	41.4 ± 0.6	48.7 ± 2.8

Table 4: *Worst-case maximal accuracies* (%) achieved by Robust-DSGD on heterogeneously-distributed CIFAR-10 with ARC and without. There are $f = 2$ (left) and $f = 3$ (right) adversarial workers among $n = 35$ workers. We consider the high heterogeneity regime $\alpha = 0.1$.

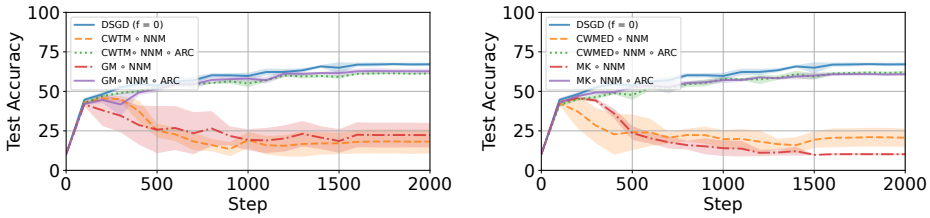

(a) CWTM and GM (b) CWMED and MK

Figure 27: Performance of Robust-DSGD when using ARC and without clipping on CIFAR-10. There are 33 honest workers and $f = 2$ adversarial workers executing the **FOE** attack. We consider the high heterogeneity regime $\alpha = 0.1$. The aggregations used are CWTM $\circ$ NNM and GM $\circ$ NNM (left), and CWMED $\circ$ NNM and MK $\circ$ NNM (right).

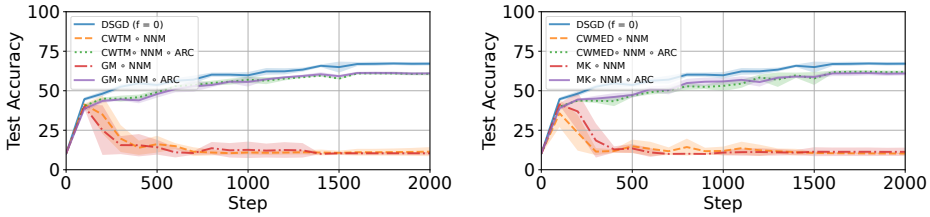

(a) CWTM and GM (b) CWMED and MK

Figure 28: Performance of Robust-DSGD when using ARC and without clipping on CIFAR-10. There are 33 honest workers and $f = 3$ adversarial workers executing the **FOE** attack. We consider the high heterogeneity regime $\alpha = 0.1$. The aggregations used are CWTM $\circ$ NNM and GM $\circ$ NNM (left), and CWMED $\circ$ NNM and MK $\circ$ NNM (right).

G.4 Comparison with Static Clipping on Fashion-MNIST and CIFAR-10

We consider three different levels of heterogeneity, that we call *moderate* (corresponding to sampling from a Dirichlet distribution of parameter $\alpha = 1$), *high* ($\alpha = 0, 1$), and *extreme* (as explained in Appendix D). These results confirm the observations made in Appendix F.

G.4.1 Fashion-MNIST

On Fashion-MNIST, we execute Robust-DSGD in a distributed system composed of $n = 15$ workers, among which $f \in \{3, 4\}$ are Byzantine. Furthermore, we train a convolutional neural network of 431,080 parameters with batch size $b = 25$, $T = 1000$, $\gamma = 0.1$, and momentum parameter $\beta = 0.9$. Moreover, the negative log likelihood loss function is used, along with an ℓ_2-regularization of 10^{-4}. See Figure 29.

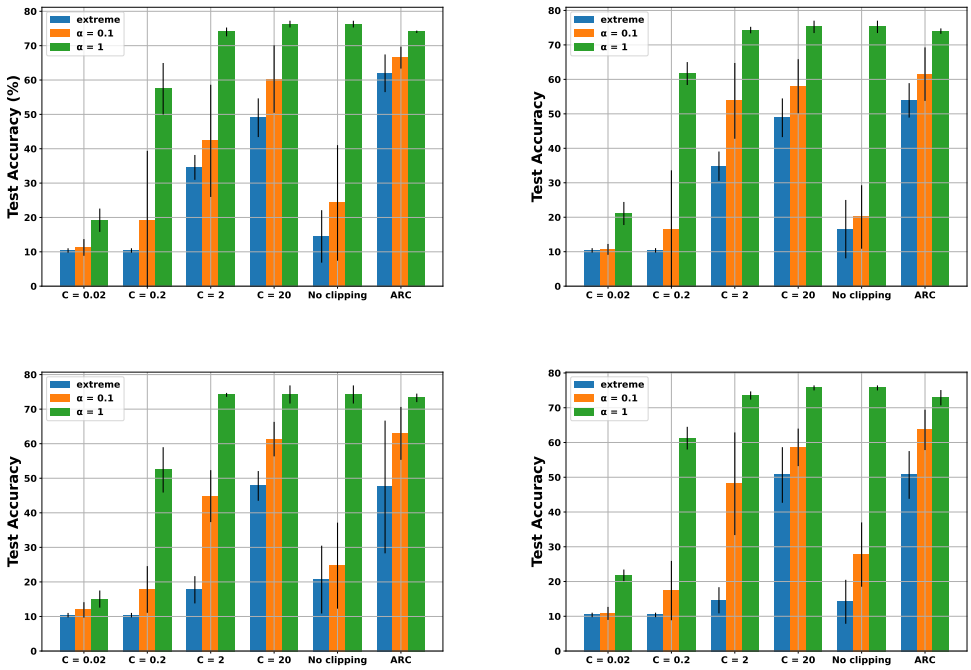

Figure 29: Impact of the clipping strategy and heterogeneity level on the worst-case *maximal* accuracy achieved during the learning against five Byzantine attacks on heterogeneous Fashion-MNIST. $f = 3$ and $n = 15$, and the heterogeneity levels considered are *extreme*, *high* ($\alpha = 0.1$), and *moderate* ($\alpha = 1$). Aggregation rules used: CWTM $\circ$ NNM (row 1, left), CWMED $\circ$ NNM (row 1, right), GM $\circ$ NNM (row 2, left), and Multi-Krum $\circ$ NNM (row 2, right). DSGD reaches accuracies 84.966%, 84.376%, 84.886% under the extreme regime, when $\alpha = 0.1$, and 1, respectively.

G.4.2 CIFAR-10

On CIFAR-10, we execute Robust-DSGD on ResNet-18 He et al. (2015), in a distributed system comprising $n = 9$ workers among which $f \in \{1, 2\}$ are Byzantine. We set $b = 128$, $T = 2000$, $\beta = 0.9$, and $\gamma = 0.1$ decaying once by $10\times$ at step 1500. Finally, we use the cross-entropy loss function with an ℓ_2 regularization of 5×10^{-4}. See Tables 5 and 6.

Attack	$C = 0.05$	$C = 0.5$	$C = 5$	$C = 50$	No clipping	ARC
FOE	26.4 ± 1.2	52.6 ± 2.0	76.4 ± 5.4	47.0 ± 8.0	43.0 ± 6.2	79.1 ± 1.6
ALIE	34.6 ± 1.3	43.3 ± 1.1	47.2 ± 3.4	47.2 ± 4.2	47.2 ± 4.2	51.8 ± 3.5
LF	33.7 ± 1.5	58.4 ± 1.8	83.6 ± 1.2	85.7 ± 0.5	85.9 ± 0.4	81.5 ± 1.4
SF	32.3 ± 1.4	57.9 ± 1.2	77.2 ± 4.6	68.6 ± 8.5	66.4 ± 9.0	82.0 ± 1.1
Mimic	38.2 ± 1.6	68.3 ± 1.4	85.6 ± 0.42	85.7 ± 0.4	85.7 ± 0.4	85.4 ± 0.5
Worst-case	26.4 ± 1.2	43.3 ± 1.1	47.2 ± 3.4	47.0 ± 8.0	43.0 ± 6.2	51.8 ± 3.5

Table 5: Maximum accuracy (%) achieved by CWTM $\circ$ NNM on CIFAR-10 under moderate heterogeneity, for various clipping strategies and attacks. There are $f = 2$ Byzantine workers among $n = 9$. We highlight in blue the highest accuracy achieved per attack (i.e., per row). See Appendix D for the full experimental setup.

Attack	$C = 0.05$	$C = 0.5$	$C = 5$	$C = 50$	No clipping	ARC
FOE	28.9 ± 1.7	56.8 ± 1.9	75.6 ± 2.8	35.5 ± 11.6	34.9 ± 12.2	75.9 ± 3.0
ALIE	34.9 ± 1.3	43.4 ± 1.0	47.4 ± 4.1	44.9 ± 3.8	44.9 ± 3.8	54.6 ± 3.6
LF	33.7 ± 1.4	58.4 ± 1.8	77.4 ± 12.9	85.8 ± 0.6	85.6 ± 0.7	80.5 ± 1.8
SF	32.5 ± 1.4	57.5 ± 1.4	77.7 ± 5.0	63.0 ± 12.0	55.4 ± 18.9	82.5 ± 0.3
Mimic	38.1 ± 1.3	68.5 ± 1.4	85.5 ± 0.5	85.9 ± 0.5	85.9 ± 0.5	85.4 ± 0.2
Worst-case	28.9 ± 1.7	43.4 ± 1.0	47.4 ± 4.1	35.5 ± 11.6	34.9 ± 12.2	54.6 ± 3.6

Table 6: Maximum accuracy (%) achieved by CWMED $\circ$ NNM on heterogeneous CIFAR-10 ($\alpha = 1$), for various clipping strategies and Byzantine attacks. There are $f = 2$ Byzantine workers among $n = 9$. We highlight in blue the highest accuracy achieved per Byzantine attack (i.e., per row).